DOI:10.14753/SE.2019.2327

Clinical relevance of vascular distribution in the palate and vestibule – establishing the theoretical foundation of novel flap designs for graft harvesting and reconstructive procedures

Ph.D. Thesis

Arvin Shahbazi Irani

School of Clinical Medicine
Semmelweis University

Supervisor:
Péter Windisch DMD, Ph.D.
Official reviewers:
Attila Szűcs DMD, Ph.D.
István Varga DMD, Ph.D.
Head of the Final Examination Committee:
Féhér Erzsébet MD, Ph.D., D.Sc.
Members of the Final Examination Committee:
Árpád Joób Fancsaly DMD, Ph.D.
Tamás Andrea MD, Ph.D.

Budapest
2019

DOI:10.14753/SE.2019.2327

TABLE OF CONTENTS

DOI:10.14753/SE.2019.2327

DOI:10.14753/SE.2019.2327

1. LIST OF ABBREVIATIONS

ASAA- Anterior superior alveolar artery

BA - Buccal artery

BDX - Bovine derived xenograft

BOP - Bleeding on probing

CAL - Clinical attachment level

CBCT - Cone beam computed tomography

CCA - Common carotid artery

CT - Computed tomography

DPA - Descending palatine artery

ECA - External carotid artery

ePTFE - expanded polytetrafluoroethylene

FA - Facial artery

FGG - Free gingival graft

GBR - Guided bone regeneration

GPA - Greater palatine artery

GR - Gingival recession

HVC - Horizontal vertical and combination

IAA - Inferior alveolar artery

ILA - Inferior labial artery

IOA - Infraorbital artery

LPA- Lesser palatine artery

MA - Maxillary artery

MEA - Mental artery

MR - Mucosal recession

NPA - Nasopalatine artery

PBS - Phosphate buffered saline

PD - Probing depth

PSAA - Posterior superior alveolar artery

SA - Submental artery

SCTG - Subepithelial connective tissue graft

SEM - Scanning electron microscopy

SLA - Superior labial artery

SUA - Sublingual artery

V - Volum

W - Weight

DOI:10.14753/SE.2019.2327

2. PREAMBLE

During my undergraduate academic years, I was impressed with the recent progression of various surgical techniques in dento-alveolar and periodontal surgeries. Between the third and fifth year of dental school, I was contributing as a teaching assistant in the Department of Anatomy, Histology and Embryology of Semmelweis University. My interest shifted towards the distribution of blood vessels and their possible influence on planning of incisions/flap designs in the oral cavity.

After my graduation, I was honored to receive an invitation to be a practice supervisor and lecturer from the English Course Director of Semmelweis University, Department of Anatomy, Histology and Embryology, Dr. Andrea Dorottya Székely, and the chair of the Department, Dr. Gábor Gerber. At the same time, I was accepted into the Dental Research Programme of the Semmelweis University School of Clinical Medicine, led by Professor Gábor Varga. The initial objective of my PhD research was to investigate the detailed analysis of blood vessels and conduct a survey in the oral vestibule and palate macroscopically, with the aim of introducing innovations related to the surgical flaps/incisions in those particular areas.

I undertook a literature search related to the morphology of blood vessel distribution in the oral cavity, collected data for a literature review and analyzed cadavers during my first year of studies under my PhD supervisor, Professor Péter Windisch, Chair of the Periodontology Department, Semmelweis University. The results of the clinical and cadaver analysis were compared to the collected data from the literature relating to the different flap/incision designs in periodontal, implant placement, bone augmentation, impacted wisdom/canine teeth, sinus floor elevation and sub-epithelial connective tissue graft surgeries. It became clear to me that the knowledge that could be gained from a pre-surgical arterial survey of anastomoses and critical points of blood distribution should be considered as one of the most important factors when designing a proper incision/flap procedure that would avoid damaging critical vessels. Such preplanned surgeries would be less invasive and attain appropriate levels of blood circulation and angiogenesis, promoting wound healing and reducing intra-operative bleeding and post-

operative complications. Therefore I started a challenging set of experiments, utilizing different visualization methods (Latex milk injection & Corrosion casting) on the vessels and dissecting them. By using these methods, I was able to convert the theoretical knowledge into practical findings and give a clear explanation about the morphological pattern of vascular distribution. During my research work, I was fortunate to be introduced to Dr. Georg Feigl, Acting Head of the Anatomy Department of the Medical University of Graz, Austria, and Dr. Bálint Molnár from the Department of Periodontology, Semmelweis University. Together with their anatomical and clinical knowledge, experience and support, we, as a team, achieved significant progress in mapping, analyzing and conducting our findings related to the course of the main arterial branches, their subdivisions and anastomoses relevant to the morphological aspects of the palate and vestibule, and their effect on clinical outcomes.

In the first phase of my PhD, I attended and assisted several surgeries utilizing different types of flap/incision design. This allowed me to clinically observe the path of blood vessels, and their possible influence on complications intraoperatively and postoperatively, under the supervision of Prof. Péter Windisch and Dr. Bálint Molnár.
I contributed as one of the co-authors to an innovative clinical research project led by Prof. Péter Windisch, which was published in a clinical case series article in the *Quintessence International Journal*. In this article, a novel split-thickness flap design without periosteal and vertical releasing incisions for horizonto-vertical ridge augmentation was introduced, with favorable wound healing due to undisturbed vascular supply.

After that, I directly investigated the theoretical findings related to the course, location and distribution of vessels on human cadavers. In the second phase of my PhD, I started to stain the blood vessels of the oral vestibule and the palate by corrosion casting and latex milk injection techniques and dissect them, in collaboration with Dr. Georg Feigl, Dr. Andrea Dorottya Székely and Dr. Gábor Gerber. We published the results of our team in the *Journal Clinical Oral Investigations*, describing the arterial supply of the palate, maxillary tuberosity and their clinical implications for flap design as well as soft tissue graft harvesting using this combination of different staining methods. We

performed the mapping of blood vessels on the hard palate and maxillary tuberosity, also discussing their influence on surgical procedures. For my publication, I was humbled to receive an award from *Apáthy István foundation,* Anatomy Department, Semmelweis University, as an appreciation of my research. After, I had an opportunity to collaborate with Prof. Péter Windisch and Dr. Bálint Molnár and contributed to the photographic illustrations of '*Gingival Recession Management'* (chapter 8: *Recession Coverage Using Autogenous Grafts*, pages 100-101 - edited by Prof. Dr. Adrian Kasaj) with some of my palate arterial distribution works. During our still-ongoing investigations, we obtained valuable new information related to the blood supply of the oral vestibule, which may contribute to a better understanding of the clinical healing patterns of vestibuloplasty and ridge augmentation procedures.

It has always been a great veneration that I have had the chance to be a member of these clinical and anatomical studies. I was involved in providing new data either for mapping of blood vessels or for applied clinical studies, such as the novel split-thickness flap. In my thesis, I want to present an overview of the related literature on the arterial distribution of the vestibule and palate. This includes anastomoses, angiogenesis, wound healing, complications and novel approaches related to the flap designs for graft harvesting on the palate, and reconstructive procedures on the vestibule. I will then present and discuss the findings from our clinical and cadaver studies.

3. INTRODUCTION

In periodontal and implant dentistry, the oral vestibule and palate are considered as target areas for various types of surgical flaps. In order to achieve successful surgical results, the knowledge of blood vessel distribution, which will affect the angiogenesis, circulation and primary wound healing, is crucial (Arnold & West, 1991; Polimeni et al., 2006). During the design of different types of incisions, the mapping of blood vessels should be acknowledged by the surgeon to avoid any complications (Kleinheinz et al., 2005; Koymen et al., 2009; Shahbazi et al., 2018).

Morphologically the vestibule presents a slit-like space which is bordered laterally by the cheeks, anteriorly by the lips and internally by the alveolar arch, gingivae and teeth (Gray & Lewis, 1918; Berkovitz et al., 2009). The gingivae are formed by dense connective tissue, tightly attached to the periosteum of the bony alveolus, and cover the cervical areas of the teeth (Gray & Lewis, 1918). They contain a complex vascular distribution. The gingivae present interdental papillae which are located coronal to the gingival margin (Berkovitz et al., 2009; Lindhe et al., 2015). In the mucosa of the vestibule, the labial glands produce fluid that empties through small ducts. Similarly, the maxillary vestibule receives the salivary secretion from Stensen's duct at the level of the upper second molar.

The oral vestibule is supplied mainly by sub-branches of the maxillary and facial arteries which are originating from the external carotid artery (ECA). The maxillary artery (MA) perfuses the upper and lower jaws including hard palate, maxillary tuberosity, maxillary sinus, vestibule, upper and lower teeth/gingivae with many branches (Rahpeyma & Khajehahmadi, 2017). These are the infraorbital artery (IOA), the greater palatine artery (GPA), the posterior superior alveolar artery (PSAA), the anterior superior alveolar artery (ASAA), the inferior alveolar artery (IAA), the buccal artery (BA) and the mental artery (MEA). The facial artery (FA) delivers different branches. The two branches of the FA which are named as, inferior labial artery (ILA) and submental artery (SA) participate in blood supply of the lower vestibule. The ILA originates at the level of the labial angle, together with the third branch, which is the superior labial artery (SLA). The course of both vessels is covered by the orbicularis

oris muscle. They move to the medial direction, give branches to the mucosa of the upper and lower vestibule, anastomose with the contralateral arteries and form the vascular network around the oral cavity (Pilsl et al., 2016). The SA passes beneath depressor labii inferioris and forms anastomoses with the ILA and mylohyoid branch of the IAA. This convoluted vascular circle, with an abundance of collateral sources of blood flow, is essential when different incisions/flaps are planned in the oral vestibule. The upper gingiva is mainly supplied by the branches coming from the PSAA, IOA, ASAA, SLA and GPA. The branches of the BA, IAA, ILA, SA and the sublingual artery (SUA) mainly supply the lower gingiva. These arteries by giving supra-periosteal branches supply the gingivae (via their terminal branches) and form meshwork with blood vessels of the periosteum and periodontal ligaments (Lindhe et al., 2015). Below the epithelium of the gingivae they build a sub-epithelial plexus which creates thin capillary loops (diameter of approximately 7 μm) in each connective tissue papilla (Lindhe et al., 2015). Below the junctional epithelium, the dento-gingival plexus (mainly formed by venules) can be found that contains small vessels without capillary loops (in healthy gingiva) (Egelberg, 1966; Lindhe et al., 2015).

The most demanding interventions in the upper/lower jaw include implant placement (Buser et al., 2013) together with a horizontal reconstruction of lost hard tissue guided bone regeneration (GBR) techniques (Donos et al., 2008; Buser et al., 2009), ridge augmentation procedures (Tinti et al., 1996; Urban et al., 2015b), sinus floor elevation (Simion et al., 2004; Niu et al., 2018), as well as periodontal pocket surgeries (Cortellini & Tonetti, 2015; Graziani et al., 2018), root coverage (Langer & Langer, 1985; Zucchelli & De Sanctis, 2000; Zucchelli et al., 2006) and vestibuloplasty (Han et al., 1995; Urban et al., 2015a) procedures. The vast majority of these surgical indications are established by full thickness mucoperiosteal flaps (Simion et al., 1998), with uni- or bilateral full thickness horizontal and vertical periosteal releasing incisions, allowing for a tension-free flap design. However, despite predictable treatment success, there are some well-known complications related to extensive flap mobilization, e.g. partial disruption of the periosteal blood supply, intraoperative haemorrhage, bone loss, partial flap necrosis, vertical scars, and shrinkage and distortion of the vestibule (Fickl et al., 2011; Lim et al., 2018). These complications may impair the final functional and

esthetic outcome of surgical interventions in both of the jaws. On the other hand, such postoperative complications after periodontal plastic surgery interventions performed with a split thickness flap design (e.g. coronally advanced flaps for root coverage procedures and vestibuloplasty procedures) are not frequently reported, possibly due to the minimally-invasive approach. Consequently, there have been several authors suggesting alternative approaches, instead of the classical mucoperiosteal flap by Tinti et al. (1996) (with two full thickness vertical and horizontal periosteal releasing incisions) for ridge augmentation procedures. These include split thickness flap designs, characterized by the absence of periosteal incisions and, hypothetically less compromised postoperative flap circulation. Hur et al. (2010) and Ogata et al. (2013) introduced a split thickness flap for ridge augmentation with one split thickness vertical incision. Windisch and co-workers (2017) published a split thickness flap design without vertical releasing incisions and with a bilaminar two-layer flap closure, and reported a low number of postoperative complications and minimal vestibular distortion following the healing period. However, detailed anatomical data are still scarce in the literature, and this might limit clinicians desiring to overcome blood supply disturbances related to various mucosal dissection techniques. Therefore, establishing a solid anatomical basis for designing surgical interventions in the vestibule by detailed mapping of the arterial pathways is needed to allow for more advanced and sophisticated surgical interventions.

Another particular area of oral and periodontal surgeries is the palate, which forms the roof of the oral cavity. The palate is divided into two parts, the hard palate (anteriorly), the soft palate (posteriorly) (Gray & Lewis, 1918; Berkovitz et al., 2009). The hard palate is bordered by the alveolar/dental arch and gingiva. As Gray & Lewis (1918) explained, the covering of the hard palate is made, “by a dense structure, formed by the periosteum and mucous membrane of the mouth, which are intimately adherent. Along the middle line is a linear raphe, which ends anteriorly in a small papilla corresponding with the incisive canal” (p. 1112). The anterior aspect of the palatal mucosa on both sides of the raphe is rough, thick and pale, but the posterior aspect is smooth, thin, and deeper in color (Gray & Lewis, 1918). The hard palate is wrapped by stratified squamous epithelium; it contains many glands which are positioned between periosteum

and mucous membrane (Gray & Lewis, 1918). Approximately from the upper second premolar toward the incisors the palate contains numerous fatty tissue, but behind the second upper premolars the palate contains more glands in its connective tissue. Generally, the suggested area for taking a subepithelial connective tissue graft (SCTG) is between the distal side of the canine to the mesial side of the first molar. The blood supply of the oral mucosa, and the palate in particular, shows a complex pattern, mainly supplied by branches of the maxillary, facial and ascending pharyngeal arteries, taking their origins from the ECA.

The third segment of the MA in the pterygopalatine fossa gives off a branch called the descending palatine artery (DPA) (Choi & Park, 2003), which descends and subdivides into the GPA and the lesser palatine artery (LPA). The GPA emerges from the greater palatine foramen, located on the hard palate between the second and third maxillary molars (Chrcanovic & Custódio, 2010; Kim et al., 2014). Further behind, on the horizontal plate of the palatine bone, the lesser palatine foramina can be found, where the branches of the LPA emerge. These arteries supply the majority of the hard palate, together with the soft palate. The branches of the GPA travel within the palatal bony groove, divided into medial and lateral palatine grooves by the palatine spine (Klosek & Rungruang, 2009; Fu et al., 2011). The medial palatine groove contains the greater palatine nerve, whereas the GPA lies in the lateral groove to supply the mucosa, periosteum and palatal gingiva (Yu et al., 2014) before entering the incisive canal to form an anastomosis with the nasopalatine artery (NPA) (Shahbazi et al., 2018). The NPA enters the incisive canal to supply the anterior region of the hard palate (i.e. intermaxillary segment). Here an anastomotic network is formed between the NPA and the GPA, supplying the majority of the palatal mucosa and periosteum.

Following oral surgical interventions, it is of high importance to be aware of the interrelation between these different anatomical entities, in order to aid the surgeon in flap design and to offer the most optimal circumstances for wound healing and revascularization. Information provided by anatomical atlases does not present clinically-relevant details of the palatal vascular network (i.e. ipsi- and contralateral anastomoses, individual changes of vascular pathways due to loss of dentition). Providing a solid anatomical basis for local characteristics of the hard palate might

enable clinicians to avoid intra- and post-operative complications when planning oral surgical interventions by optimizing incision and flap designs. In order to elevate a flap, which allows surgical intervention to be followed by undisturbed wound healing, accurate information regarding the size and division of muscular, mucosal and periosteal vasculature is necessary. Oral cavity vestibule needs predictable surgical care due to the numerous vascular distribution in movable mucosa, keratinized gingiva and the periosteum.

The course of blood vessels in the palate and oral vestibule has a significant influence on the result of reconstructive surgical interventions by affecting intraoperative haemorrhage and postoperative healing. There are several surgery types of maxillofacial/oral surgical or periodontal treatment for which a well-established knowledge of secure incision lines and surgical approaches would be highly beneficial: harvesting of SCTG (Langer & Calagna, 1980; Langer & Langer, 1993; Benninger et al., 2012), free gingival graft (FGG) (Sullivan & Atkins, 1969; Edel, 1974; Oh et al., 2017), removal of impacted canines (Abrams et al., 1988; Köşger et al., 2009), and flaps to allow implant placement (Kleinheinz et al., 2005; Koymen et al., 2009). Among all surgical interventions in the oral cavity, especially the front maxilla/mandible, requires predictable surgical care because of plausible esthetic commotion following surgeries disrupting the vestibular circulation. Although the morphological features of vestibular and palatal structures have previously been thoroughly investigated, clinicians still frequently face anatomical challenges during surgeries, and there is a growing need for a comprehensive macroscopical mapping of the palatal mucosal blood supply in order to avoid dangerous intraoperative and postoperative complications (Harris et al., 2005; Griffin et al., 2006).

According to the literature, investigation of the blood flow in oral mucosa can be performed by in vivo angiography (Mörmann & Ciancio, 1977), laser Doppler or laser speckle analysis (Hoke et al., 1994; Molnár et al., 2017). These approaches provide valuable clinical data on functional changes in blood circulation following thermal, mechanical or chemical stimuli, and might be used for monitoring postoperative wound healing patterns following oral surgery or periodontal surgery interventions. Nevertheless, these in vivo approaches are only capable of providing indirect

information on blood vessel function and structures. Thus more accurate ex vivo macro- and microscopical investigations are required to achieve a solid anatomical background for the physiological observations made by blood flow analysis methods.

Several staining methods exist that might be used to visualize the blood vessels of the palate for macroscopical analysis, such as latex milk injection (Alvernia et al., 2010) or corrosion casting (Rueda Esteban et al., 2017). These can all be used in human cadavers by injecting a substance through the ECA.

Latex milk is a flexible material, and it is composed of proteins, resins, tannins, oils, sugars, alkaloids and gums. (Haenssgen et al., 2014). It endures as an emulsion of polymer micro-particles which is mixable with water (Haenssgen et al., 2014). In general, the colored latex milk is injected into the vessels to analyze the path of the branches and sub-branches of the different vessels. This material is kept in an alkaline medium and will solidify when it is converted to an acid medium. The latex becomes solidified when it dries out. Also, by applying high pressure or keeping the latex under low temperature, it can become hardened as well. The latex hardens rapidly in the presence of formalin (Bergeron et al., 2006), this process is called *emulsion polymerization* (Haenssgen et al., 2014). After a proper embalming period of the cadaver by Thiel's solution and flushing of the vessels, they are injected with the latex milk. Thiel's solution has no detectable odor and results in life-like flexibility of body parts, excellent color preservation of muscle and vasculature, as well as superior antimicrobial preservation of cadavers (Thiel, 1992a; Thiel, 1992b; Thiel, 2002; Ottone et al., 2016). The addition of diluents can modify the viscosity and the setting time of latex (Alvernia et al., 2010; Haenssgen et al., 2014). Diluents for latex can be water (Alvernia et al., 2010; Haenssgen et al., 2014), ammonium hydroxide (NH_4OH), or triethylamine ($(C_2H_5)_3N$) (Thiel, 1992b; Haenssgen et al., 2014).

The corrosion casting method uses solidifying material such as methacrylates in order to discover the three dimensional structure of blood vessels within the tissue (Hossler & Douglas, 2001; Haenssgen et al., 2014). In particular, the methacrylates are monomers in polymer plastics and can create the acrylate polymers, that are elastic, lucid and defiant to breakage (Haenssgen et al., 2014). In this method, the injection process is

suggested to be performed on fresh specimens, which are without any previous fixation or formalin (Rueda Esteban et al., 2017). Having a fresh corpse is essential before casting in order to prevent complications in the steps of the injection due to solidification and retraction, mainly in vascular tissues (Rueda Esteban et al., 2017). After casting procedures, the corrosion, dissection, washing and drying will be the next steps before achieving the final outcome. The vessels can be identified during dissection. In addition, the latex milk and corrosion casting display excellent architecture when the specimen is to be X-rayed or studied under a microscope.

4. OBJECTIVES

The goal of my PhD dissertation is two-fold: firstly, I evaluate the existing evidence available in the literature related to the analysis of blood vessel distribution and their clinical relevance in the palate and oral vestibule. Secondly, I present novel information related to flap/incision designs in hard- and soft tissue reconstructive surgeries. The current available novel findings might affect the incision techniques in soft tissue graft harvesting in the future. Available data related to the pattern of mapping and subdivisions of the vessels have raised a number of fundamental questions regarding the possible future clinical impact of the presented novel flap/incision designs for ridge augmentation procedures. My research is focused on establishing the methodological basis to develop proper incision/flap designs, as well as angiogenesis, reduced complications with intra operative bleeding, wound healing and other post-operative problems. My PhD research in clinical and human cadaver studies was conducted to find answers to the main question: *How can an incision/flap, designed according to accurate anatomical knowledge of the vascular distribution, contribute to acceptable angiogenesis, wound healing and less intraoperative bleeding beyond current therapeutic approaches?*

The clinical and human cadaver studies were performed with the following aims:

- To introduce a novel surgical technique without damaging the collateral blood vessels, together with reconstruction of lost hard and soft tissues around dental implants, describing a partial thickness flap design with predictable two layer periosteal-mucosal wound closure.
- To establish a detailed macroscopic mapping of the anastomoses of the vestibular and palatal blood vessels by applying anatomical methods on cadavers, in order to bridge the gap between basic structural and empirical clinical knowledge.
- To provide clinicians with a good basis to understand the anatomical background of intra- and postoperative complications, as well as early wound healing events in SCTG and proper incision/flap design, depending on anatomical location.

5. MATERIALS AND METHODS

The present thesis reports on a clinical study (I) and a human cadaver research study (II), which are summarized. The clinical case report study was conducted at the Department of Periodontology, Semmelweis University, and involved patients undergoing treatment of alveolar hard and soft tissue defects. Cadaver research was carried out at the Department of Anatomy, Histology and Embryology, Semmelweis University, Budapest, Hungary and the Department of Macroscopical and Clinical Anatomy, Medical University of Graz, Austria.

Summary of study I (clinical/case report study)

Case report analyses of three patients (2 females, 1 male) which were 52-63 years of age with generalized chronic periodontitis presented posterior partial edentulism with class C alveolar defects according to the horizontal, vertical and combination (HVC) classification. A novel split thickness flap for guided bone regeneration was applied without vertical releasing incision to maintain the blood vessels. The flap was buccally and lingually mobilized in a full thickness manner. After removal of the granulation tissues simultaneously, a bone block was fixed supracrestally into prosthetically determined implant sites and implants were inserted. Harvested autogenous bone with a xenograft were mixed and grafted to the deficient areas. A nonresorbable titanium membrane was trimmed and adapted over the grafted area. The lingual flap and the buccal periosteal layer were sutured with horizontal mattress sutures. The buccal mucosal layer was sutured above the periosteal layer with horizontal mattress sutures. Noninterrupted sutures were added on the flap margins to achieve complete primary closure. Soft tissue augmentation at membrane removal was applied in two of the patients. Following abutment connection, fixed implant-retained partial dentures were fabricated (Windisch et al., 2017).

Summary of study II (human cadaver study)

a. Ten head specimens from Austrian cadavers (six males, four females, two edentulous, eight dentate, 43-95 years of age) were prepared for analysis of vascular pathways of the oral vestibule (mucosa and periosteum) with their clinical impact on incision and flap design in oral surgery and implant dentistry. In this study most of the cadavers were injected with latex milk (manuscript under preparation).

b. Ten head specimens from six Hungarian cadavers (three males, three females; one dentate, five edentulous, 65-84 years of age) and four Austrian cadavers (two males, two females; two dentate, two edentulous, 59–90 years of age) were prepared for the macroscopic analysis of the blood vessels supplying the palatal mucosa. Their clinical implications for flap design and soft tissue graft harvesting were inspected. Four cadavers were stained with the corrosion casting method and the other six cadavers with latex milk injection (Shahbazi et al., 2018).

The corpses were fixed with Thiel's solution. The ECAs were dissected. In both techniques, before injection, the vessels were rinsed with phosphate buffered saline (PBS) and other solutions. Then careful injection was continued.

5.1 Study I (clinical/case report study)

Three nonsmoking patients with generalized chronic periodontitis were treated: a 63-year-old woman (Case 1), a 52-year-old man (Case 2), and a 56-year-old woman (Case 3). Patients presented posterior partial edentulism (Applegate-Kennedy Class II, mandible; Class I, mandible; Class II, mandible, respectively) with class C alveolar defects according to the horizontal, vertical and combination (HVC) classification (Wang & Al-Shammari, 2002). In each case, non contained periodontal defects were found at neighboring teeth (mandibular right first premolar, one-wall defect; mandibular right first premolar, one-wall defect; mandibular right canine, one-wall defect, respectively). Patients presented good general health, completed initial periodontal treatment, and maintained proper oral hygiene. Full mouth plaque and bleeding scores were less than 20% in all cases prior to surgeries.

The patients were treated in full accordance with ethical principles, including the World Medical Association Declaration of Helsinki (version 2008). Retrospective evaluation and publication of pre- and postoperative clinical and radiographic data was approved by the Semmelweis University Regional and Institutional Committee of Science and Research Ethics (Approval Number: 77/2011). Surgical interventions were undertaken with the understanding and written consent of each subject.

5.1.1 Treatment approach

In all three cases, horizonto-vertical ridge augmentation utilizing a novel split-thickness flap design was performed to ensure optimal three-dimensional implant positioning and long-term stability of peri-implant hard tissues. The same surgical technique was utilized in all cases: implant placement with a simultaneous ridge augmentation procedure. If optimal peri-implant soft tissue stability could not be ensured upon thinned alveolar mucosa, hard tissue reconstruction was followed by additional soft tissue grafting at membrane removal. Following abutment connection, fixed implant-retained partial dentures were fabricated (Windisch et al., 2017).

5.1.2 Case 1

- Local anesthesia (Ultracain DS Forte, Sanofi-Aventis) was given.
- A midcrestal incision on the edentulous ridge was extended by intrasulcular incisions at two neighboring teeth for additional mobilization to ensure tension-free wound closure.
- On the lingual side, a full-thickness flap was elevated down to the level of the mylohyoid line. Subsequently, inserting muscles and fibers were released from the inner aspect of the flap by blunt dissection, resulting in buccal displacement of the lingual flap.

- On the buccal side, the flap was elevated in full thickness from the midcrestal incision up to the mucogingival junction. Subsequently, flap elevation was continued in partial thickness by blunt dissection towards in the apical direction. Inserting muscles were released from the intact periosteum, resulting in a tension-free mobilization of the buccal partial-thickness flap.

- No vertical releasing incisions were made in order to avoid collateral periosteal blood supply disturbance.

- After granulation tissue removal, exposed root surfaces were scaled and planed by means of hand and ultrasonic instruments.

- The vertical and horizontal positioning of the fixtures was determined by means of a prefabricated prosthetic guide.

- After drilling with a proprietary predrill (Screw system, Hager & Meisinger), a bone block fixation screw was inserted 3 mm supracrestally into one of the prosthetically determined implant sites.

- Subsequently, a 3-mm-high bone cylinder was retrieved by a trephine bur (Hager & Meisinger) from the same site. The previously inserted block fixation screw was included in the retrieved cylinder. The diameter of the trephine did not exceed the diameter of the last twist drill (inner diameter 2.5 mm/outer diameter 3.5 mm) used for subsequent implant osteotomy.

- After bone cylinder retrieval, at implant insertion, fixtures were left to protrude up to 3 to 5 mm from the crestal bone.

- Cover screws were placed.

- The previously harvested autogenous bone cylinder was fixed onto the alveolar ridge by screwing down the included bone block fixation screw 3 mm following pre-drilling to achieve further buccal and vertical tissue support in the inter-implant area. Thus, fixtures and the supracrestally fixed bone cylinder served as space maintainers outlining the three-dimensional extent of hard tissue reconstruction.

- Supracrestal implant surfaces were covered by locally retrieved autogenous bone particles using bone scrapers (Buser #1/2, Hu-Friedy). Since the amount of harvested autogenous bone was not sufficient to fill the created supracrestal defect completely, a bovine-derived xenograft (BDX; Bio-Oss, particle size 0.25 to 1.0mm, Geistlich) was used as additional grafting material.

- Autogenous bone and BDX were mixed in a 1:2 ratio. Subsequently, a nonresorbable titanium membrane (FRIOS Bone Shield, Dentsply Friadent) was trimmed and adapted over the grafted area, fixed by titanium pins (FRIOS Membrane Tacks, Dentsply Friadent).

- Following membrane fixation, as a result of the increased flap elasticity due to horizontal extension, the buccal periosteal layer and lingual flap could be coronally mobilized to achieve complete closure above the membrane.

- The lingual flap and the buccal periosteal layer were sutured with orally positioned horizontal mattress sutures (4/0 Supramid, Braun; “periosteal sutures”).

- The buccal mucosal layer was sutured to the oral flap above the periosteal layer with buccally positioned horizontal mattress sutures (5.0 Supramid, Braun; “mucosal sutures”).

- Finally, flap margins were adapted with noninterrupted sutures (6.0 Supramid, Braun; “marginal sutures”) to achieve complete primary closure. If possible, all sutures were placed in keratinized mucosa. If the width of the keratinized mucosa did not allow, then the periosteal and mucosal sutures were placed approximately 2 mm from the incision line into nonkeratinized mucosa.

- Nine months postoperatively, soft tissue augmentation was carried out upon insufficient mucogingival conditions. Proper implant soft tissue coverage could not be ensured because of thinned alveolar mucosa following the augmentation procedure (underlying titanium membranes became transparently visible). The width and thickness of keratinized tissue was less than 2 mm over the grafted area, as confirmed by direct intraoperative measurements. Therefore, soft tissue augmentation was

performed during stage-two surgery 9 months after ridge augmentation and implant placement. The same flap design was applied as for the augmentation procedure. Flap elevation was, however, only minimally extended to allow for membrane and titanium pin removal.

- A free connective tissue graft was harvested from the palate using the single incision technique (Hürzeler & Weng, 1999) and sutured to the lingual full-thickness flap by horizontal mattress sutures (5/0 Supramid, Braun).
- Then, the vestibular mucosal layer was mobilized to achieve full coverage over the connective tissue graft. Oral and buccal flaps were adapted with mattress and non-interrupted sutures as described above.
- Three months after soft tissue augmentation, bone block fixation screws and cover screws were removed following elevation of a minimally invasive partial-thickness flap.
- Healing abutments were connected.
- The mucosal layer of the buccal partial-thickness flap was sutured to the oral flap by horizontal mattress sutures (5/0 Supramid, Braun) without primary wound closure in the inter-implant areas. Secondary epithelialization of these areas resulted in the formation of new keratinized tissue.

5.1.3 Case 2

- The surgical protocol followed the same technique as described in Case 1.
- Due to the favorable horizontal dimensions of the alveolar ridge, a larger diameter bone cylinder could be retrieved (diameter of trephine bur: inner diameter 3 mm, outer diameter 4 mm).
- A sufficient amount of autogenous bone particles could be locally harvested to be used as the sole filling material without the need for the application of any BDX.

- Connective tissue grafting was not indicated, since the width and thickness of keratinized tissue exceeded 2 mm over the grafted area.

- For the abutment connection, the same surgical approach was utilized as described in Case 1. Titanium membranes, titanium pins, bone block fixation screws and cover screws were removed at abutment connection, i.e. 9 months following ridge augmentation and simultaneous implant placement.

5.1.4 Case 3

- The surgical protocol followed the same technique as described in Case 1, except that two bone cylinders (inner/outer diameter: 3/4 mm and 2.5/3.5 mm) were retrieved.

- The expanded polytetrafluoroethylene (ePTFE) suturing material (CV5, Gore) was used as periosteal suture (Fig. 1, 2).

- The connective tissue grafting was indicated, since the width and thickness of keratinized tissue was less than 2 mm over the grafted area, as confirmed by direct intraoperative measurements. Soft tissue augmentation was conducted in a similar manner to Case 1 over the grafted area. For the abutment connection, the same surgical approach was utilized as described in Case 1.

- The titanium membrane, titanium pins and cover screw were removed at abutment connection, i.e. 9 months following ridge augmentation and simultaneous implant placement.

5.1.5 Post-operative maintenance

- Patients were not allowed to wear partial removable dentures on the operation site during the whole healing period of 9 months.

- Postoperative care consisted of 0.2% chlorhexidine mouth rinse (Corsodyl, GlaxoSmith- Kline) twice a day for 4 weeks.

- Mucosal and marginal sutures were removed 5 to 7 days after surgery, periosteal sutures 10 to 14 days after surgery.
- Patients were not allowed to brush or chew at operation sites for 14 days after surgery.
- Patients were recalled for professional tooth cleaning twice a week in the first 2 weeks postoperatively, and once a month until second surgery.
- Neither subgingival instrumentation nor periodontal probing was performed during this time interval.
- Screw-retained fixed partial dentures were placed 4 weeks after abutment connection.
- After prosthetic loading of implants, patients were recalled as part of supportive periodontal therapy every 6 months for professional oral hygiene.

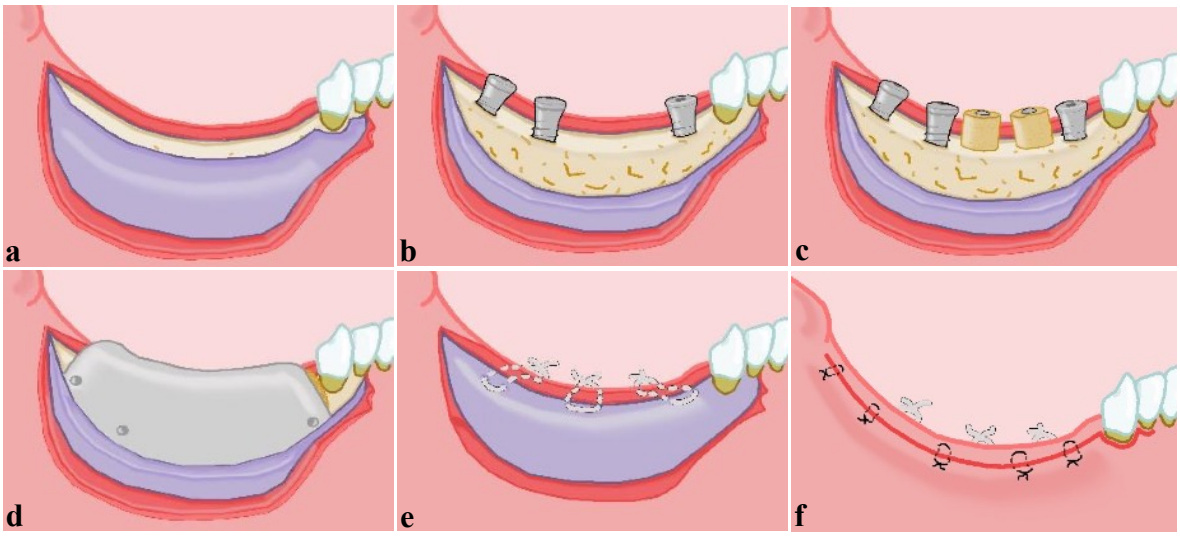

Fig. 1 Surgical treatment approach.

a) Split thickness flap preparation, **b)** Supracrestal implant positioning, **c)** Placement of bone cylinders, **d)** Fixation of titanium membrane, **e)** Periosteal suturing, **f)** Mucosal suturing.

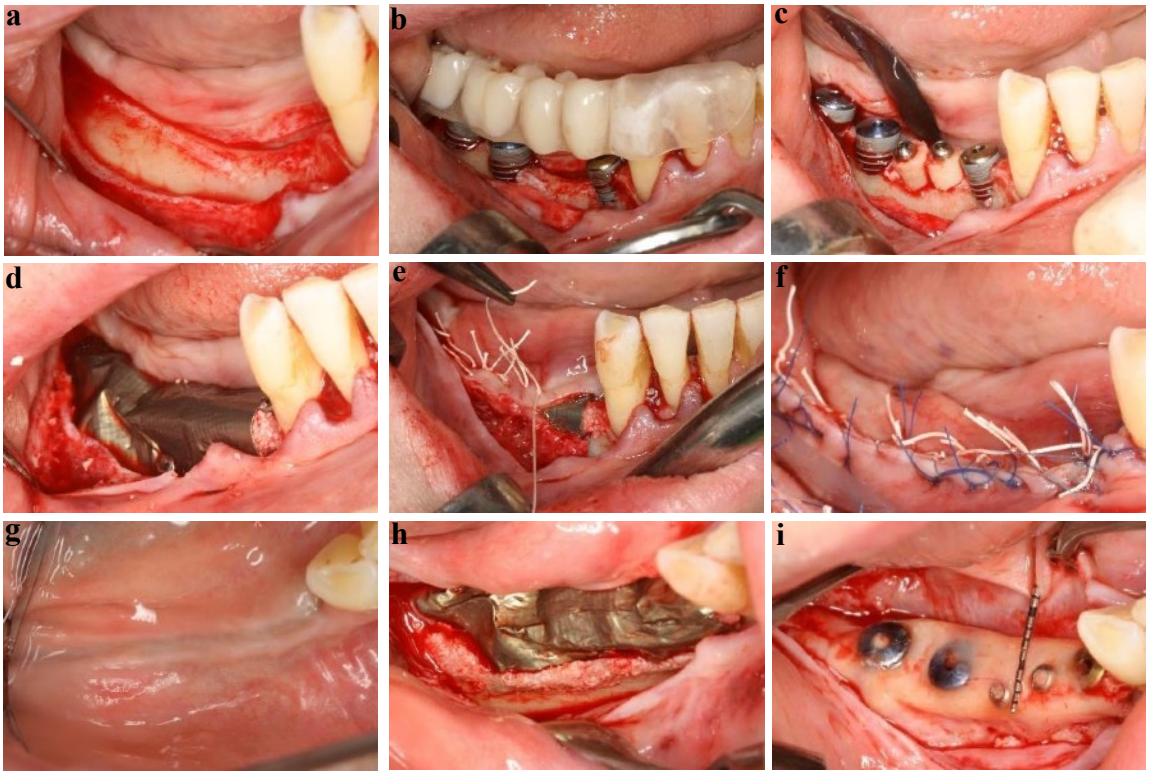

Fig. 2 Surgical treatment approach for horizontovertical ridge reconstruction (Case Three). **a)** Split thickness flap preparation, **b)** Supracrestal implant positioning, **c)** Placement of bone cylinders, **d)** Fixation of titanium membrane, **e)** Periosteal suturing, **f)** Mucosal suturing, **g)** Healing at 9 months, **h)** Re-entry and membrane removal at 9months, **i)** 9 months intraoperative view, complete defect reconstruction.

5.1.6 Clinical evaluation

At the time of the augmentation procedure and abutment connection, direct intraoperative measurements were registered to evaluate hard tissue formation around the implants. At each implant, the distance between the top of the implant shoulder and the alveolar crest was measured at four sites (mesial, distal, oral, vestibular aspect) at baseline (i.e. subsequent to implant placement) and at 9 months, i.e. immediately after membrane removal. All intraoperative measurements were recorded using a standard periodontal probe (UNC 15, Hu-Friedy). The thickness of keratinized mucosa over the grafted area was measured at baseline and 9 months following the augmentation procedure via sterile Kerr-files. All clinical measurements were rounded to the nearest 0.5 mm. Follow-up measurements were performed at 12, 24, 36, 48, and 60 months

after prosthetic loading. Probing depth (PD), mucosal recession (MR), and bleeding on probing (BOP) were recorded around implants. PD, gingival recession (GR), and clinical attachment level (CAL) were recorded at neighboring natural teeth preoperatively and 9 months later to evaluate the outcome of the horizontally extended flap design involving teeth adjacent to the reconstructed ridge.

Periodontal measurements were also performed on a yearly basis during the follow-up period for 60 months; PD was less than 4 mm in each site (data not shown).

5.1.7 Radiographic evaluation

Panoramic radiographs were recorded at baseline. To assess crestal bone changes, intraoral radiographs were taken at baseline, immediately after surgeries, as well as at abutment connection and 12, 24, 36, 48, and 60 months after prosthetic loading. Images were digitized, and the distance between implant shoulder and the crestal bone was measured at the mesial and distal aspects of each fixture. Digital images were examined under an 8-fold magnification. Implant height was used for calibration. In Case 1, conventional computed tomography (CT) analysis was made prior to augmentation; in Cases 2 and 3, cone beam CT (CBCT) analysis was performed. In all three cases, additional CBCT analysis was performed 9 months postoperatively. Only qualitative radiographic evaluation was performed on CT scans.

5.2 Study II (human cadaver study)

The methods of latex milk injection (fourteen specimens) and corrosion casting (six specimens) were used bilaterally on human cadavers. These were donated to the Department of Anatomy, Semmelweis University, Budapest, Hungary, according to Hungarian approval rules of anatomical donation, and to the Department of Anatomy of the Medical University of Graz, Austria, complying with the Anatomical Donation Program of the Medical University of Graz and in accordance with the Austrian law. The course and distribution of blood vessels in relation to soft and hard tissues, used in combination with a layer-by-layer dissection protocol, were studied. Digital

photographs were taken of each specimen from multiple directions with a magnification range of 1:1 to 1:3 using a macro lens mounted to a digital single lens reflex camera equipped with a ring light (Canon 600D, Canon 100 mm 2.8 macro lens, Canon MR-14 EX ring light). Photographs were analyzed by visual inspection on a calibrated monitor at 1:1 magnification.

5.2.1 Latex milk injection

Latex milk stains the blood vessels and makes them macroscopically remarkable. It facilitates the dissection of the vessels. By this method, the anatomical and physiological relation of blood vessels can be analyzed (Alvernia et al., 2010). In this method, the cadavers can be fixed in Thiel solution (Thiel, 1992a; Thiel, 1992b; Thiel, 2002) tanks for about a year. This solution permits prolonged preservation, keeps the natural color, texture, plasticity and flexibility of the tissues, same as a fresh specimen, and it allows easier injection of vessels till the thinnest branches (Thiel, 1992a; Thiel, 1992b; Thiel, 2002; Ottone et al., 2016).

5.2.1.1 Thiel solution

Since ancient times, the goal of preservation of the body has existed. This was mainly due to religious and scientific reasons. In 1992, Walter Thiel introduced a novel method which allowed the preservation of the body with natural colors.

The Thiel's technique is composed of two steps:

1) Intravascular injection formula.

2) Fixation of the cadavers for a determined period in immersion solution inside a sealed container to disinfect, preserve tissue plasticity and avoid dehydration without the usage of preservation fluid (Thiel, 1992a; Thiel, 1992b; Thiel, 2002; Ottone et al. 2016). By this method, the cadaver handling is more effective, and it eludes the formation of vexatious gases because of low formaldehyde concentrations used in the solution (Thiel, 1992a; Thiel, 1992b; Thiel, 2002; Ottone et al. 2016) (Table 1).

Table 1 Basic chemical components used in the Thiel embalming method.

Name of chemical component	Effect of chemical component
4-chloro-3-methylphenol ($ClC_6H_3(CH_3)OH$)	*Fixation of the cadavers*
Ammonium nitrate (NH_4NO_3)	*Fixation of the cadavers*
Potassium nitrate (KNO_3)	*Fixation of the cadavers*
Sodium sulfate ($Na_2SO_{4)}$	*Fixation of the cadavers*
Boric acid (H_3BO_3)	*Disinfection of the cadavers*
Ethylene glycol ($C_2H_6O_2$)	*Preservation of tissue plasticity*
Hot water (H_2O)	*Softening of stained tissues*
Formaldehyde (CH_2O)	*Disinfection, tissue fixation and embalming agent*

The carotid arteries were washed with an intravascular Thiel solution, "containing 14300 mL of solution A, plus 500 mL of solution B and the addition of 700 g of sodium sulfite as well as 300 mL formalin" (Ottone et al., 2016, p. 1443) for an average body weight of 80 kg (Table 2). Then, the cadavers were injected with the latex milk, or they were fixed for around 6 months in the immersion solution (Table 2 and 3). The specimens were retained in *zipper polyethylene bags* and they were used for a long time (Thiel, 1992b; Thiel, 2002; Ottone et al., 2016). The outcomes of the utilization of the Thiel solution were non-irritating, almost odorless, maintaining the color and flexibility of the cadavers (Thiel, 1992a; Thiel, 2002; Ottone et al., 2016). The specimens were comparable to the living body, with adequate temporomandibular joint mobility and maintained tissue elasticity which were suitable for surgical interventions (Ottone et al., 2016). After embalming of the cadavers for about 6 months, those head specimens which were not injected by latex milk previously, were ready for the next step, which was latex milk injection.

Table 2 Basic composition of injection and immersion solutions described by W. Thiel in 1992. Note: Adapted from "Walter Thiel's Embalming Method. Review of Solutions and Applications in Different Fields of Biomedical Research" by Ottone NE, Vargas CA, Fuentes R, Del Sol M, 2016, Int. J. Morphol, 34, p.1443. Copyright 2016 by Nicolás Ernesto Ottone; Claudia A. Vargas; Ramón Fuentes; Mariano del Sol (INTERNATIONAL JOURNAL OF MORPHOLOGY), Attribution-NonCommercial, (https://creativecommons.org/licenses/by-nc/4.0/deed.en) CC BY-NC 4.0.

Solution A	***Injection solution***	***Immersion solution***
Boric acid 3 g	Solution A 14300 ml	Ethylene glycol 10 ml
Ethylene glycol 30 ml	Solution B 500 ml	Formaldehyde 2 ml
Ammonium nitrate 20 g	Formaldehyde 300 ml	Solution B 2 ml
Potassium nitrate 5 g	Sodium sulfate 700 g	Boric acid 3 g
Hot water 100 ml		Ammonium nitrate 10 g
Solution B		Potassium nitrate 10 g
Ethylene glycol 10 ml		Sodium sulfate 7 g
4-chloro-3-methylphenol 1 ml		Hot water 100 ml

The process of latex milk injection together with the dissection of the blood vessels in the oro-maxillofacial region was technique-sensitive. The equipment and chemicals to be used in latex milk injection were strictly checked and measured (Table 4). Any mistake or improper functioning of equipment would damage the entire process and the macroscopic analysis of the vessels.

Table 3 Calculation of the percentage of weight/volume (w/v), and percentage of volume/volume (v/v) used in the immersion solution (according to Thiel, 1992a; Thiel, 1992b; Thiel, 2002; Ottone et al., 2016).

Chemical component	**% w/v or % v/v**
Boric acid	3 % (w/v)
Ethylene glycol	10 % (v/v)
Ammonium nitrate	10 % (v/v)
Potassium nitrate	5 % (w/v)
Sodium sulfite	7% (w/v)
Formalin	2 % (v/v)
Solution B	2 % (v/v)

Table 4 Equipment and chemical components, with their functional properties, used for latex milk injection.

Equipment or chemical	Function
Catheter (Foley, Coude)	*Conducts different vascular solutions and the latex milk into the blood vessels*
Fiber plastic bands	*Prevents from any back flow or leakage of latex milk (isolation)*
Electrical chemical mixer	*Mixes the chemical components*
Pressure pump (compressor) / syringe	*Pumps the latex milk into the blood vessels*
Phosphate buffered saline (PBS) (alkaline solution)	*Rinses the vessels Removes clots that blocks the passage of latex milk*
Liquid latex	*Stains and solidifies the blood vessels*
Color agent	*Coloring agent of blood vessels (red for the arteries, blue for the veins)*
Ammonia (NH_3)	*Clears the vessels and removes clots*

5.2.1.2 Process of latex milk injection

- The carotid trigones were carefully dissected. The common carotid arteries (CCAs), and subsequently the ECAs, were gently revealed.
- The CCA/ECA was rinsed with PBS under the pressure of minimum 27 kPa, and then perfusion of Thiel's solution via the CCA/ECA was performed.
- Following perfusion with Thiel's solution, the arteries were subsequently flushed again with PBS.
- Indirect anatomical study of the arterial orientation during irrigation with PBS through the CCA/ECA was made.
- After embalming, the CCA/ECA was cannulated carefully with either a Foley or a Coude catheter. A proper sized catheter was chosen.

- Then the catheter was placed in the CCA/ECA. The fixation of the catheter was made precisely to prevent any leakage of the substance under pressure. The fixation (isolation) was performed by alternating knots (with fiber plastic bands) on different aspects of the vessel.

- Prior to injection of latex, 20-30 ml of diluted ammonia (NH_3) was injected to clear the vessels.

  Note: According to Echt (1998), ammonia can be used as a *'preservative'* in the latex because it agitates the molecules of rubber and provides a two-phase product consisting of 30 - 40% solids; the product can be concentrated to 60% solids, producing ammoniated latex concentrate, that includes 1.6% ammonia by weight. By usage of low-ammonia latex concentrate (0.15 - 0.25% ammonia) and adding of secondary preservatives such as Sodium pentachlorophenate (C_6Cl_5ONa), Tetramethylthiuram disulfide $(CH_3)_2NCSS_2CSN(CH_3)_2$, Sodium dimethyldithiocarbamate ($C_3H_6NNaS_2$) and Zinc oxide (ZnO) the *coagulation* and *contamination* can be avoided (Echt, 1998).

- The latex milk (Creato Latexmilch, Zitzmann Zentrale, Baden, Germany) was colored red and it was injected by the pressure pump, syringe or pasteurized bottle with a delivery tube into the arteries. During the injection, the same and constant pressure is sufficient, but a higher pressure can be used to provide a complete distribution into the finer vessels.

- These arteries were "full form" and capable of resisting the rigidity of dissection thereafter. About 150 ml of latex was sufficient for an adult cadaver injection. After 20-30 min of injection, the latex started to solidify and imparted a red color to the arteries.

- Cadaver head specimens were ready for dissection about 4-6 weeks following injection, during which the latex would have time to set. Cadavers were sealed in plastic bags for a certain period with anti-fungal agents.

- After the embalming period, the specimens were dissected under 2.5x magnification using Nr. 15 and Nr. 15C surgical blades. The mucosa was elevated, the injected vessels were dissected in each layer, and the path of the arteries, along with their network, were macroscopically examined.

5.2.2 Corrosion casting

The method was mainly followed according to Lametschwandtner et al. (1990), Verli et al. (2007), and Rueda Esteban et al. (2017). This process, associated with or without scanning electron microscopy (SEM) is utilized to investigate the vascular orientation of organs and tissues (Lametschwandtner et al., 1990; Verli et al., 2007). The corrosion casting involves two main distinct procedures:

- **Casting:** Formation of the casts by the vessel lumens and solidification of vessels with a low-viscosity resin (Hodde et al., 1990; Lametschwandtner et al., 1990; Verli et al., 2007; Rueda Esteban et al., 2017). Casting reveals the complexity of blood vessels in three-dimensions in relation to bony anatomical landmarks as a result of complete maceration of soft tissues (Verli et al., 2007; Haenssgen et al., 2014, Shahbazi et al., 2018). The most crucial aspects of this method are the usage of head cadavers 1-2 days post mortem, isolation and selection of high quality vascular casting material (Table 5).

- **Corrosion:** Maceration of tissues with an alkaline solution surrounding the polymerized resin (Hodde et al., 1990; Lametschwandtner et al., 1990; Sims & Albrecht, 1993; Verli et al., 2007). This process can be conducted by Sodium hydroxide (NaOH) and Potassium hydroxide (KOH) solutions, with/without detergents, at various concentrations (Hodde et al., 1990; Lametschwandtner et al., 1990; Sims & Albrecht, 1993; Verli et al., 2007; Rueda Esteban et al., 2017). The method results in the total dissolution of soft tissues located around the previously-casted vessels.

Table 5 Criteria for vascular casting materials (according to Verli et al., 2007).

Low viscosity
Polymerization time: 3-15 min
No shrinkage during polymerization
Maintaining the structural configuration while drying
Small particles to fill the capillaries
Permiting quantitative analysis
No morphological alterations in the tissues and vessels
No penetration of tissues and their interstitial spaces
Resistant to the corrosion process
Permitting microdissection
No damage to the surrounding tissues
Atoxic

The corrosion casting is more technique-sensitive than the latex milk injection, so the equipment, chemical components (Table 6) and freshness of the specimen should be strictly controlled. It is suggested that the cadavers without any previous fixation or formalin injection to be selected (Rueda Esteban et al., 2017). This method indicates a solidification in vascular tissues, so precise rinsing with water for several minutes is essential to eliminate clots and increase the visibility of the blood vessels (Rueda Esteban et al., 2017). After careful dissection of carotid trigones, the ECAs are rinsed with heparin or hydrogen peroxide (H_2O_2) and then by PBS which are described in pre-casting phase.

Table 6 Equipment and chemical components, with their functional properties, used in corrosion casting.

Equipment, chemical components	Function
Catheter (Foley, Coude)	*Conducts different vascular solutions and the polymer into the blood vessels*
Multifilament 2-0 suture	*Prevents leakage of the injected material under pressure*
Pressure pump (compressor) / syringe	*Pumps the polymer into the blood vessels*
Clamp (Kelly, Rochester)	*Inhibits the formation of bubbles and polymer reflux from the vessel during injection*
Stainless-steel container	*Conserves the specimen during corrosion*
Air exposure / Incubator / Drier / Freezing	*For drying*
Phosphate buffered saline (PBS) (alkaline solution)	*Flushes the vessels* *Removes debris*
Heparin	*Anticoagulant* *Removes clots*
Hydrogen peroxide (H_2O_2)	*Anticoagulant* *Removes clots*
Thiel's solution/ Glutaraldehyde ($C_5H_8O_2$)/ Formaldehyde (CH_2O) or Paraformaldehyde ($HO(CH_2O)_nH$)	*Prefixation vascular solutions*
Coloring agent	*Coloring agent of blood vessels* *(red for the arteries, blue for the veins)*
Acrylic resin, methyl-methacrylate	*Polymer-mixed with the coloring agent and injected to the blood vessels*
Sodium hydroxide (NaOH)	*For corrosion*
Potassium hydroxide (KOH)	*For corrosion*
Water / 5% formic acid (CH_2O_2) or Collagenase associated hydrochloric acid (HCl)	*For Submersion of the corroded specimen*
Alcohol	*Immersion solution, during evaporation, promotes a low surface tension in the specimens*

DOI:10.14753/SE.2019.2327

5.2.2.1. Process of corrosion casting

5.2.2.1.1. Pre-casting phase

- Careful preparation of the specimen, dissection and identification of the CCA/ECA was performed and then isolation (Hill & McKinney, 1981) was made.

- After choosing the proper sized catheter/tube (Foley or Coude), which would allow the injection of the polymer, it was fixed very securely into the CCA/ECA. The size of the tube was depending on the vessel that was going to be injected. It was preferred to use the same or slightly smaller sized tubes for the injection. Once the tube was positioned in the artery, any leakage of the injected material under pressure was avoided by *transfixation suture* (Rueda Esteban et al., 2017), with alternating knots on each side of the artery (Fig. 3). Based on suggestion of Rueda Esteban et al. (2017), multifilament 2-0 sutures were used. This suture prevented knot loosening and leakage of the polymer during the injection. Also, in some cases, for further isolation dental floss was used as well. Due to the high probability of damaging the arteries during injection, this process was carried carefully.

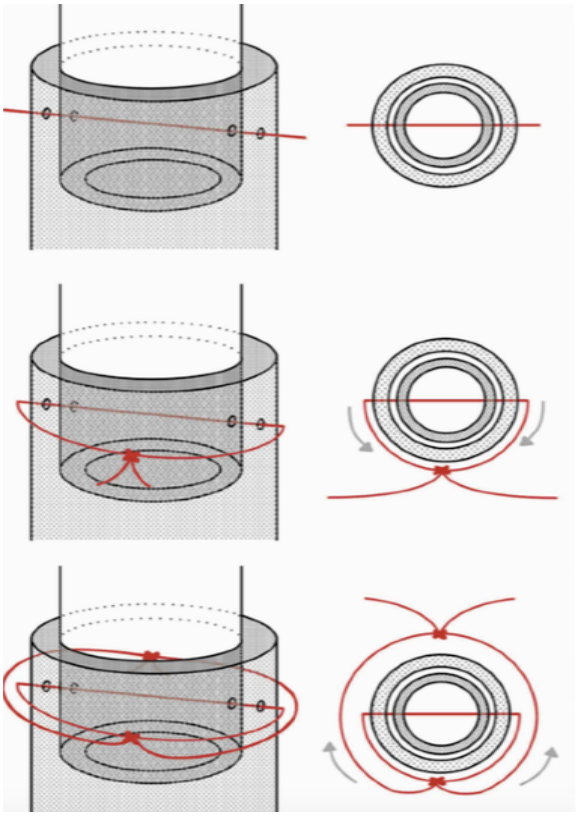

Fig. 3 Suggested suture pattern for cannulation. Note: Adapted from "Corrosion Casting, a Known Technique for the Study and Teaching of Vascular and Duct Structure in Anatomy" by Rueda Esteban RJ, López McCormick JS, Martínez Prieto DR, Hernández Restrepo JD, 2017, Int. J. Morphol, 35, p.1150.

- Administration of anticoagulants; heparin or hydrogen peroxide (H_2O_2) (1-2%) were essential to remove clots that could otherwise meddle with the polymer's entry, to expedite the injection (Lametschwandtner et al., 1990; Hodde et al., 1990; Verli et al., 2006; Rueda Esteban et al., 2017). After using H_2O_2, it was crucial to wash the vessels with the water, due to production of foam which would influence sufficient injection, the compound and could harm surrounding tissue (Rueda Esteban et al., 2017).

- ECAs were flushed by PBS under the pressure of minimum 27 kPa to clean away debris.

- Vascular prefixation with Thiel's intravascular solution was performed after flushing (Shahbazi et al., 2018). Based on literature glutaraldehyde ($C_5H_8O_2$), formaldehyde (CH_2O) and paraformaldehyde ($HO(CH_2O)_nH$) at various concentrations (Hodde et al., 1990; Selliseth & Selvig, 1995; Ojima et al., 1997; Verli et al., 2007) could be used, to evade resin extravasating from the vessels into the tissues (Lametschwandtner et al., 1990), to promote withstanding of vascular walls (Selliseth & Selvig, 1995) and to reduce vascular expansion throughout injection of the resin (Kishi et al., 1990; Verli et al., 2007).

- Following prefixation, spontaneous washing with PBS solution was required, to withdraw the fixative and increase resin penetrability.

- To enhance the clarity of the injected polymer in the blood vessels, a red color code was given to differentiate the arteries.

5.2.2.1.2. Casting phase

- Acrylic resin (methyl-methacrylate) was selected as a polymer to be injected into the ECA. Before injection it was noted, as the resin viscosity decreases, the polymerization shrinkage increases, so if the resin would be diluted then the probability of shrinkage would be higher (Lametschwandtner et al., 1990).

- After preparing 150 ml of polymer (Acrifix 2R0190, Evonik Performance Materials GmbH, Darmstadt, Germany), which contained red color agent (So-Strong red color tint, Smooth-on, Inc. Easton, United States), it was injected directly into each tube. As Lametschwandtner et al. (1990) and Verli et al. (2007) suggested, to gain a homogeneous cast, the injection must be performed with a proper speed, so higher speed would result in rupture of the arteries and lower speed would result in incomplete injection. The injection was made with different sized syringes. Following recommendation of Rueda Esteban et al. (2017) in case that, "one injection is not enough a clamp should be placed on the tube - remove the syringe plunger - refill the syringe and then remove the clamp and resume the injection immediately to avoid the formation of bubbles or polymer reflux" (pp. 1149-1150).

- The tubes were sealed with proper clamps such as Kelly/Rochester and then particular time was required for the polymerization process (Rueda Esteban et al., 2017). When the casting with the resin was made, to keep the *in vivo* shape of the vessels without contortions, the head specimens were not moved for at least 30 min (Lametschwandtner et al., 1990; Verli et al., 2007; Rueda Esteban et al., 2017). Subsequently, the specimens were washed in a warm water at a temperature of 40 - 60◦ C for around 30 min - 24 h to achieve full polymerization of the resin (Lametschwandtner et al., 1990; Verli et al., 2007). This process needed accurate handling of materials by the investigators operating on the specimen.

5.2.2.1.3. Corrosion phase

- The tissue surrounding the cast (polymer) was dissolved (macerated) by sodium hydroxide (NaOH) and potassium hydroxide (KOH) solutions at a concentration of 2-4% (Hodde et al., 1990; Sims & Albrecht, 1993). We mainly used KOH. This reaction could work at room temperature, but in order to achieve faster results, the head specimens were macerated at 40◦C (Lametschwandtner et al., 1990) up to 60/70◦C (Shahbazi et al., 2018). According to suggestion of the Rueda Esteban (2017), since the NaOH (or even KOH) could penetrate aluminum or iron containers

at high temperature, the process was conducted in a *stainless-steel* container. The maceration was performed by KOH/NaOH solution for approximately 8-14 days.

- We used PBS for debris removal. In order to improve the visualization of the vascular structures, the areas of interest were washed with PBS for several minutes.

- In the final phase a careful dissection of the main vessels with the surrounding tissues were performed. During the tissue removal, it was crucial to save the three-dimensional structure of small terminal branches without any hazard.

- Before starting the drying, the corroded head specimens were immersed in water (Ojima et al., 1997) for 5 - 30 min. Other suggested solutions for this step are (according to the literature):
  - 5% formic acid (CH_2O_2) solution (Selliseth & Selvig, 1993).
  - Collagenase associated hydrochloric acid (HCl) solution (Motoyama & Watanabe, 2001).

- There are several methods to dry the specimens such as drying at room temperature by air exposure, freezing and/or using an incubator (Lametschwandtner et al., 1990). Since the air exposure at the room temperature for the head specimens was a simple drying method, it was used. According to Lametschwandtner et al. (1990) and Verli et al. (2007), One of the drawbacks of this method is the high tension that the vascular network surface carries when the water evaporates. In order to reduce surface tension during drying, it is suggested by the literature that the specimens be submerged in solutions which contain high concentrations of alcohol that upon evaporating, allow a low surface tension (Lametschwandtner et al., 1990; Selliseth & Selvig, 1995; Verli et al. 2007).

- After removal (dissection) of the surrounding tissues, the arteries with a minimum diameter of 200 μm were stained and analyzed.

6. RESULTS

6.1. Study I

6.1.1. Post-operative findings

The healing procedure after surgeries was uneventful in all cases, without any serious local or systemic adverse events. Only moderate post-operative swelling was observed, no membrane exposure occurred until membrane removal. In Case 1 and Case 3, 9 months postoperatively the midcrestal vertical thickness of the alveolar mucosa decreased to less than 2 mm. Thus, in Case 1 and Case 3, connective tissue grafting was performed, and abutment connection followed 3 months later. Healing of the donor site and the grafted area occurred without complications, the midcrestal thickness of keratinized mucosa increased to more than 2 mm 3 months after soft tissue grafting. In Case 2, the midcrestal vertical thickness of the alveolar mucosa exceeded 2 mm immediately before membrane removal, and so soft tissue grafting was not indicated. After 9 months of healing, complete pocket resolution without gingival recession was observed at sites with periodontal attachment loss. CAL, PD, and GR measurements at adjacent teeth are summarized in Table 7.

6.1.2. Intraoperative findings at membrane removal

Following membrane removal, a non-mineralized periosteal-like layer was seen on top of the reconstructed alveolar crest, which was partially removed to allow for abutment connection. Implants were clinically stable in all cases. New hard tissue formation was confirmed by visual assessment and probing. The vertically and horizontally enlarged alveolar ridge displayed a similar clinical appearance to neighboring native bone in all cases. Implant surfaces and bone block fixation screws were completely covered by newly formed hard tissues (Fig. 4).

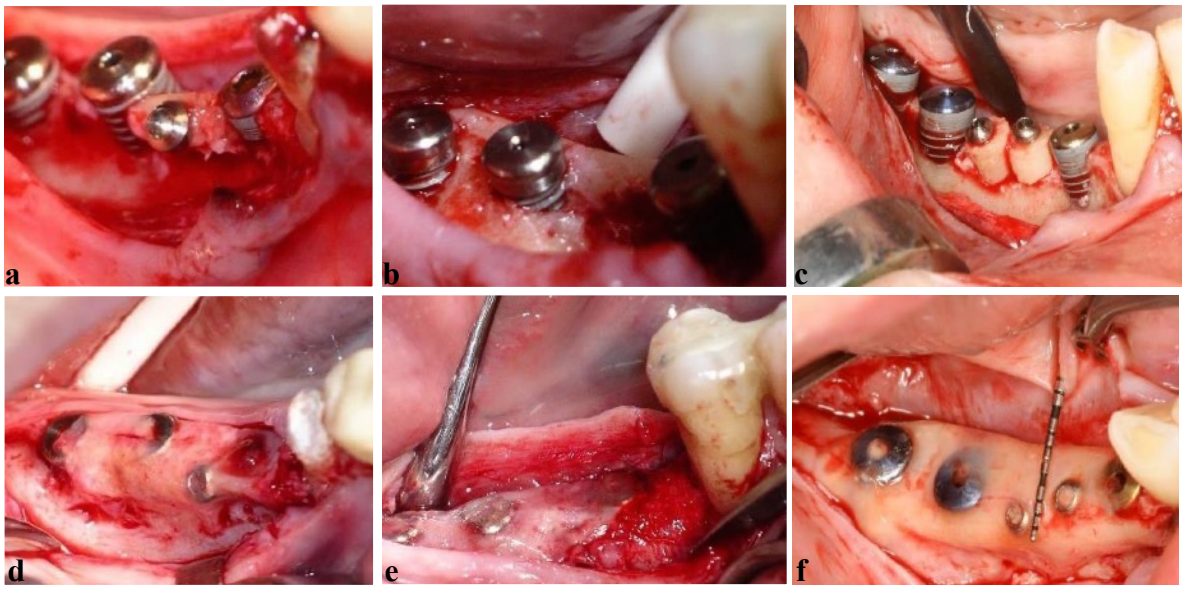

Fig. 4 Intraoperative changes demonstrating complete defect reconstruction.
a) Case 1 – Implant placement, **b) Case 2** – Implant placement, **c) Case 3** – Implant placement, **d) Case 1** – 9 months defect fill, **e) Case 2** – 9 months defect fill, **f) Case 3** – 9 months defect fill.

A comparison of the mean bone to implant/screw contact at first surgery and at membrane removal demonstrated a mean crestal bone regeneration of 3.08 ± 1.25 mm. Direct clinical measurements around implants are summarized in Table 8.

After 4 weeks of soft tissue healing, implants were prosthetically loaded. At regular follow-up visits of 12, 24, 36, 48, and 60 months after prosthetic loading, peri-implant PD did not exceed 4 mm in any of the cases. Neighboring teeth previously receiving periodontal regenerative treatment also showed maintenance of PD, GR, and CAL recorded at implant loading (data not shown). In Cases 1 and 3, no soft tissue recession occurred, whereas in Case 2, 1 mm of recession was detected on the lingual aspect of the inserted implants. A high level of oral hygiene was maintained throughout the follow up period. Neither BOP nor absence of keratinized mucosa were detected in any of the cases. Prosthetic complications did not occur.

Table 7 Periodontal changes at neighboring teeth: neighboring teeth initial pocket probing depth (PD), clinical attachment level (CAL) and gingival recession (GR), and changes in PD, GR, CAL (mm) of neighboring teeth 9 months postoperatively are shown.

Case	Tooth surface	PD	CAL	GR	ΔPD	ΔCAL	ΔGR
One	45 db	2	3	1	0	0	0
	45 dl	2	2	0	0	0	0
Two	44 db	7	10	3	4	3	-1
	44 dl	4	6	2	2	2	0
Three	43 db	3	6	3	1	2	1
	43 dl	2	3	1	0	0	0

Table 8 Peri-implant crestal bone level changes: inserted implants and uncovered implant surfaces, changes in vertical dimensions (Mesial: Vertical M, Distal: Vertical D, Vestibular: Vertical V, Oral: Vertical O) (mm), changes in horizontal dimensions (Vestibular: Horizontal V, Oral: Horizontal O) (mm) after 9 months postoperatively.

Case	Implant position	Uncovered surfaces	Vertical M	Vertical D	Vertical V	Vertical O	Horizontal V	Horizontal O
One	46	3	0	2	2	3	2	1
	47	4	4	4	4	4	3	1
	48	4	3	2	3	2	2	1
Two	45	4	4	3	5	2	2	3
	46	4	3	2	3	1	3	3
	47	4	3	3	3	1	2	3
Three	44	4	1	3	5	3	2	1
	46	4	5	4	5	4	2	2
	47	4	3	5	4	3	2	2

DOI:10.14753/SE.2019.2327

6.1.3. Intraoral radiographs outcomes

On intraoral radiographs taken immediately after surgery, the border between native crestal bone and grafting material could be clearly identified, as well as contours of the titanium membrane, titanium pins, and bone block fixation screws. Nine months postoperatively, on intraoral radiographs taken prior to membrane removal, harvested autogenous bone and xenograft particles could not be distinguished from the earlier native bone margins. At 12 months after prosthetic loading, signs of positive bone remodeling and crestal bone maintenance were similar, as shown on intraoral radiographs in all cases, despite the fact that different grafting materials were used. Moreover, radiographic results showed maintained alveolar crest contours at 60 months follow-up in all three cases (Fig. 5).

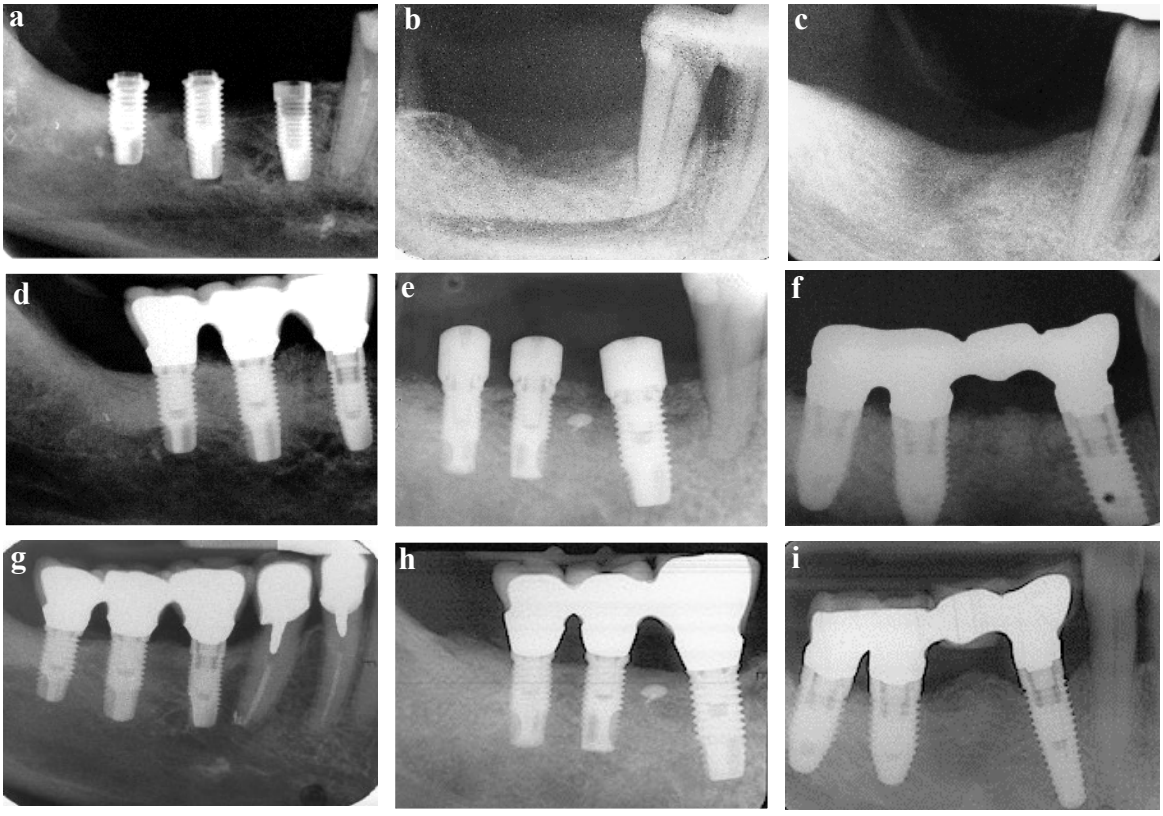

Fig. 5 Long term radiographic follow up of crestal bone maintenance.
a) Patient 1 – implant insertion, **b) Patient 2** – baseline, **c) Patient 3** – baseline, **d) Patient 1** – implant loading, **e) Patient 2** – abutment connection, **f) Patient 3** – implant loading, **g) Patient 1** – 5 years follow-up, **h) Patient 2** – 5 years follow-up, **i) Patient 3** – 5 years follow-up.

6.1.4. Cone beam computed tomography outcomes

Nine month postoperative CBCTs demonstrated successful hard tissue reconstruction (Fig. 6). Fixtures were surrounded by dense radio-opaque areas resembling native alveolar bone, and remaining xenograft particles could not be distinguished from adjacent bone. In all cases, thickening of the outer cortical layer of mandibular bone was observed.

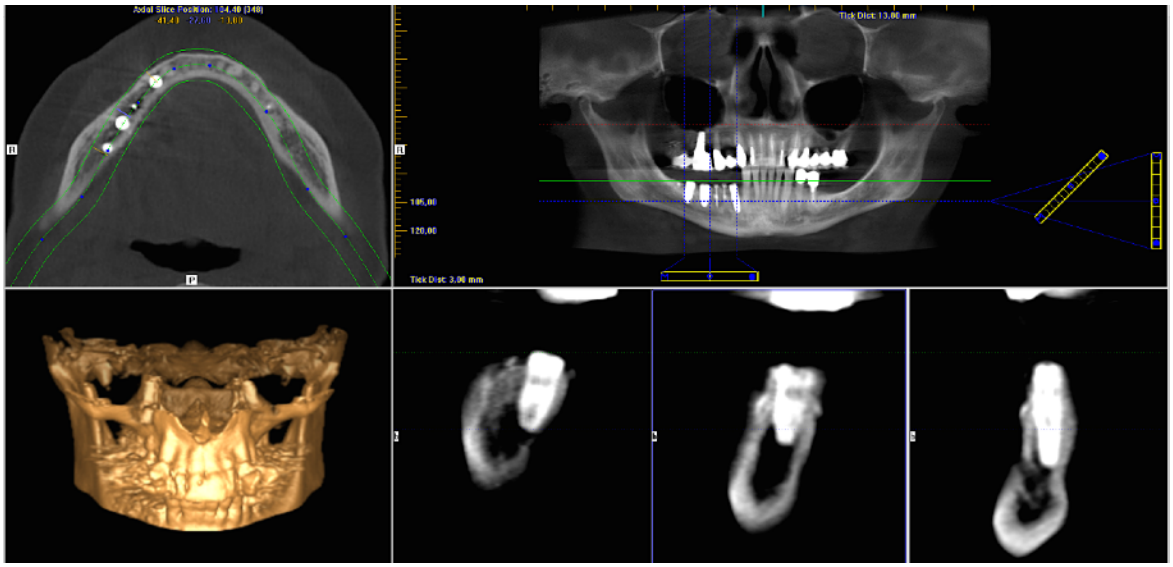

Fig. 6 Postoperative cone beam computed tomography (CBCT) outcome of case 1 after 9 months (lower right quadrant), representing hard tissue reconstruction with simultaneous implant placement.

6.2. Study II

6.2.1 Results of the vascular survey analysis in the vestibule

At the vestibule of the anterior maxilla, in the most superficial mucosal layer, main vertical arteries with transverse anastomoses were detected prior to dissection (Fig. 7, 8). In the anterior surface of the maxilla the vertical vessels coming from the SLA and IOA repeatedly divided below the mucogingival junction, and terminal arteries further descended towards the mesial and distal aspect of each papilla in dentate cadavers (Fig. 8). Opposed to the anterior maxilla, main arteries were horizontally orientated in the molar area of the posterior maxilla, but vertical branches were observed too (Fig. 8).

DOI:10.14753/SE.2019.2327

Each of the main vertical and the bifurcated sub-branches were anastomosed with adjacent vessels through horizontal branches. In the lower vestibule the transverse course of ILA originating at the level of lower first molar was successfully presented (Fig. 9). At the vestibule of the anterior mandible, vertical branches were received from the ILA. Among these vessels many horizontal anastomoses were detected, and a higher density of superficial mucosal vessels were observed at the area of premolars and molars (Fig. 9). These arteries supply the mucosa and the periosteum of the anterior mandible together with the sub-branches of the SA.

Fig. 7 Vascular distribution of the upper vestibule. **a)** Demonstration of the superior labial artery (SLA) with its superficial vertical branches, which are bifurcating and form anastomoses with each other and supply the mucosa and frenulum of the anterior maxilla. **b)** Superficial branches of the posterior superior alveolar artery (PSAA) and infraorbital artery (IOA).

DOI:10.14753/SE.2019.2327

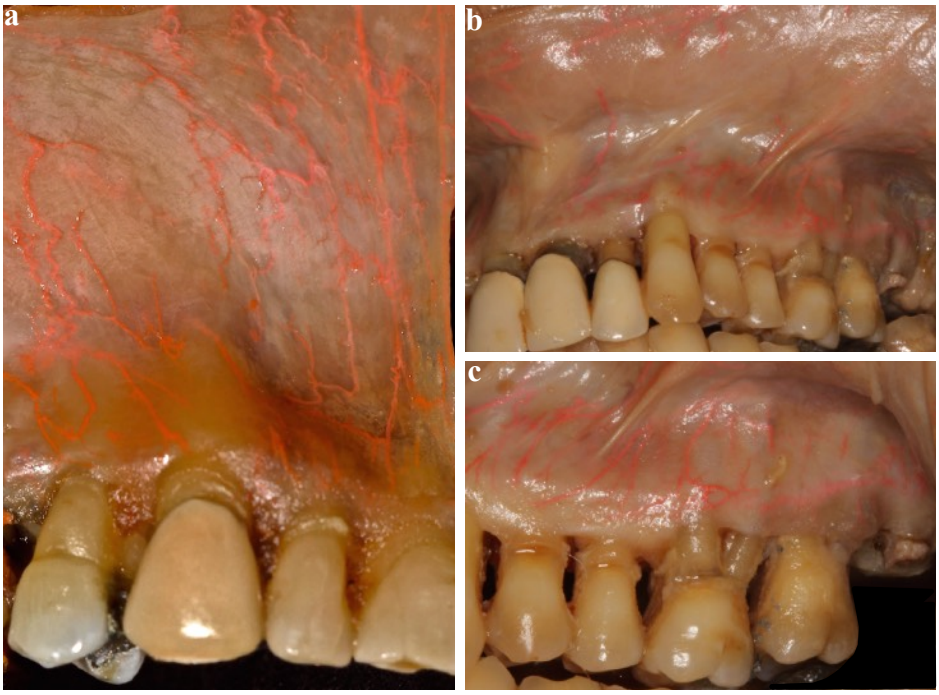

Fig. 8 Pathway of the blood vessels on the upper vestibule. **a)** Vertically-oriented blood vessels originating from superior labial artery (SLA) and infraorbital artery (IOA) move toward the papilla. **b)** Overview picture from the direction of the vessels in the mucosa of the maxillary vestibule. **c)** Magnified picture at the level of the upper molars. The posterior superior alveolar artery (PSAA), moves in a horizontal direction and sends vertical branches and these branches follow the same pattern as anterior maxilla.

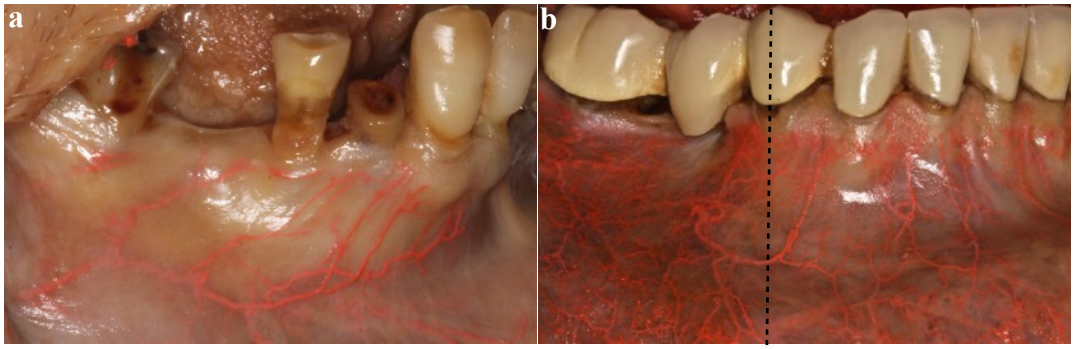

Fig. 9 Vascular survey of the lower vestibule. **a)** The oblique course of inferior labial artery (ILA) (at the level of first-second lower premolar) with its main vertical sub-branches are seen as they move toward the papillae and bifurcate to form a circulatory network in the lower gingiva. **b)** Superficial sub-branches with a complex pattern of anastomoses, deriving from the ILA and submental artery (SA). The vertical path of the vessels from the level of the mucogingival junction toward the papillae are observed. At the premolar and molar areas a higher density of vessels were detected.

6.2.2 Results of the vascular survey analysis in the palate and maxillary tuberosity

The course of the greater palatine artery was clearly presented by applying corrosion casting and latex milk injection techniques, the former showing the complete mapping of blood vessels along with osseous surroundings, the latter allowing for layer-by-layer dissection and demonstration of the soft tissue environment. Major and secondary branches of the GPA and it's relation to the palatine spine, variation in division of the sub-branches, different anastomoses with NPA, LPA as well as with contralateral branches of the GPA, were recorded (Fig. 10, 11,12). A complex arterial circle network were stained and recorded in the superficial and the periosteal layers (Fig. 10, 11,12). Another important finding of cadavers with an edentulous upper jaw revealed that due to the resorption of the bone, the GPA developed a curvy pathway, especially at the area of the molars-premolars (Fig. 13). Also, some penetrating intraosseous branches at the premolar-canine area were observed (Fig. 14). The blood supply around the maxillary tuberosity was also presented (Fig. 15). As soon as the greater palatine artery emerges out from the greater palatine foramen, it sends one or two branches toward the tuberosity. Also, the lesser palatine artery sends one or two branches forming anastomoses to this area (Fig. 15). The above-mentioned findings are summarized in Figure 16, which clearly demonstrates the complexity of the palatal blood supply. At the level of the 2nd molars the distance of the GPA branches from the gingival margin was 11.3 ± 0.9 mm on average (ranging from 10 to 13 mm) (Fig. 17). In all the cadavers, a high amount of adipose and dense connective tissues were detected, together with numerous vessels. In those cadavers showing signs of obesity, an increased amount of adipose tissue was observed in the posterior palate compared to cadavers without signs of obesity.

DOI:10.14753/SE.2019.2327

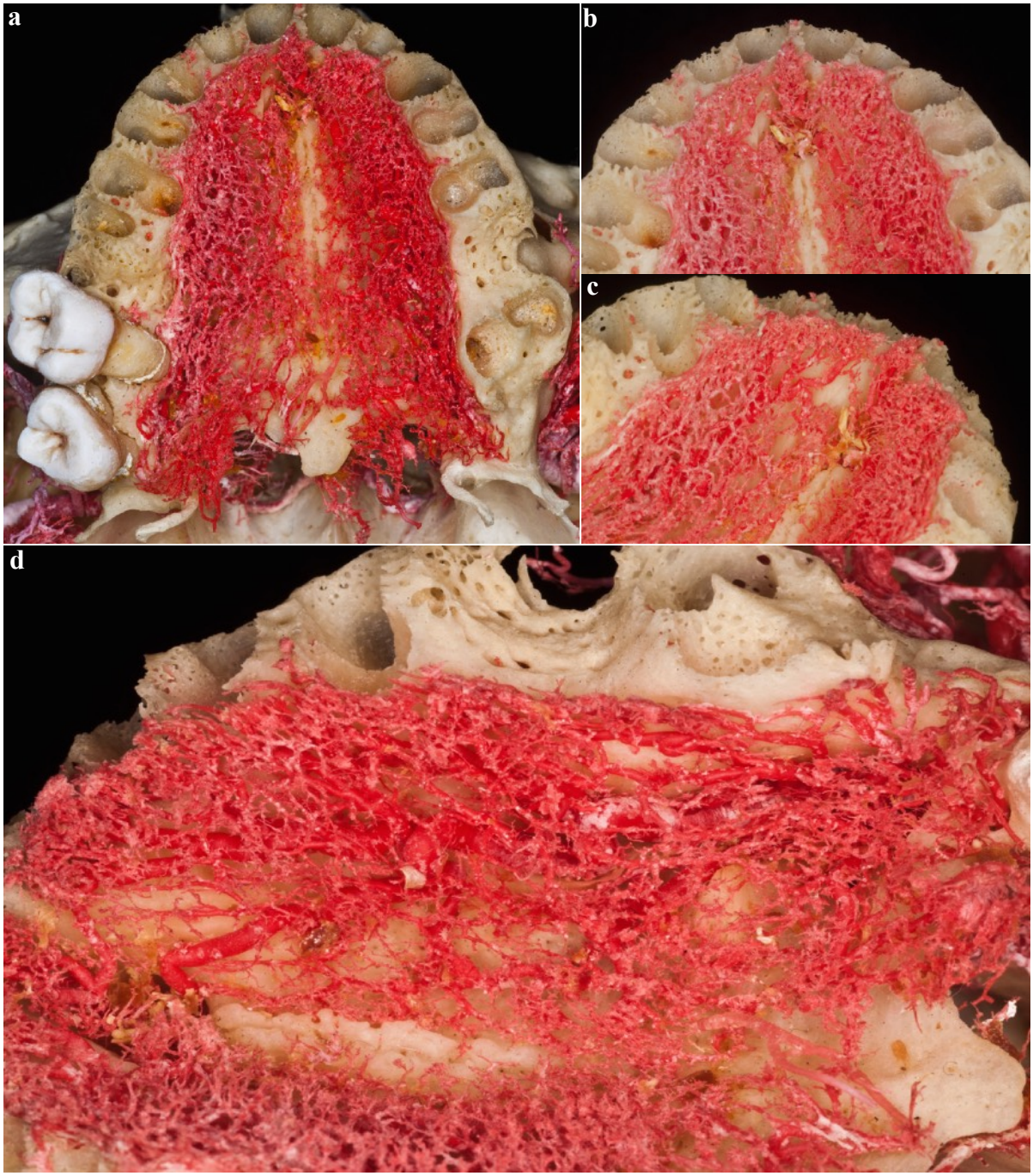

Fig. 10 Blood supply of the palate, by the greater palatine artery (GPA), the lesser palatine artery (LPA) and the nasopalatine artery (NPA), together with the anastomoses between the GPA and NPA shown by corrosion casting. **a)** Overview of the palatal blood supply. **b)** Anastomosis between the GPA and the NPA. **c)** Blood supply of the pre-maxilla by the NPA and the GPA. **d)** Course of the GPA and its branches.

DOI:10.14753/SE.2019.2327

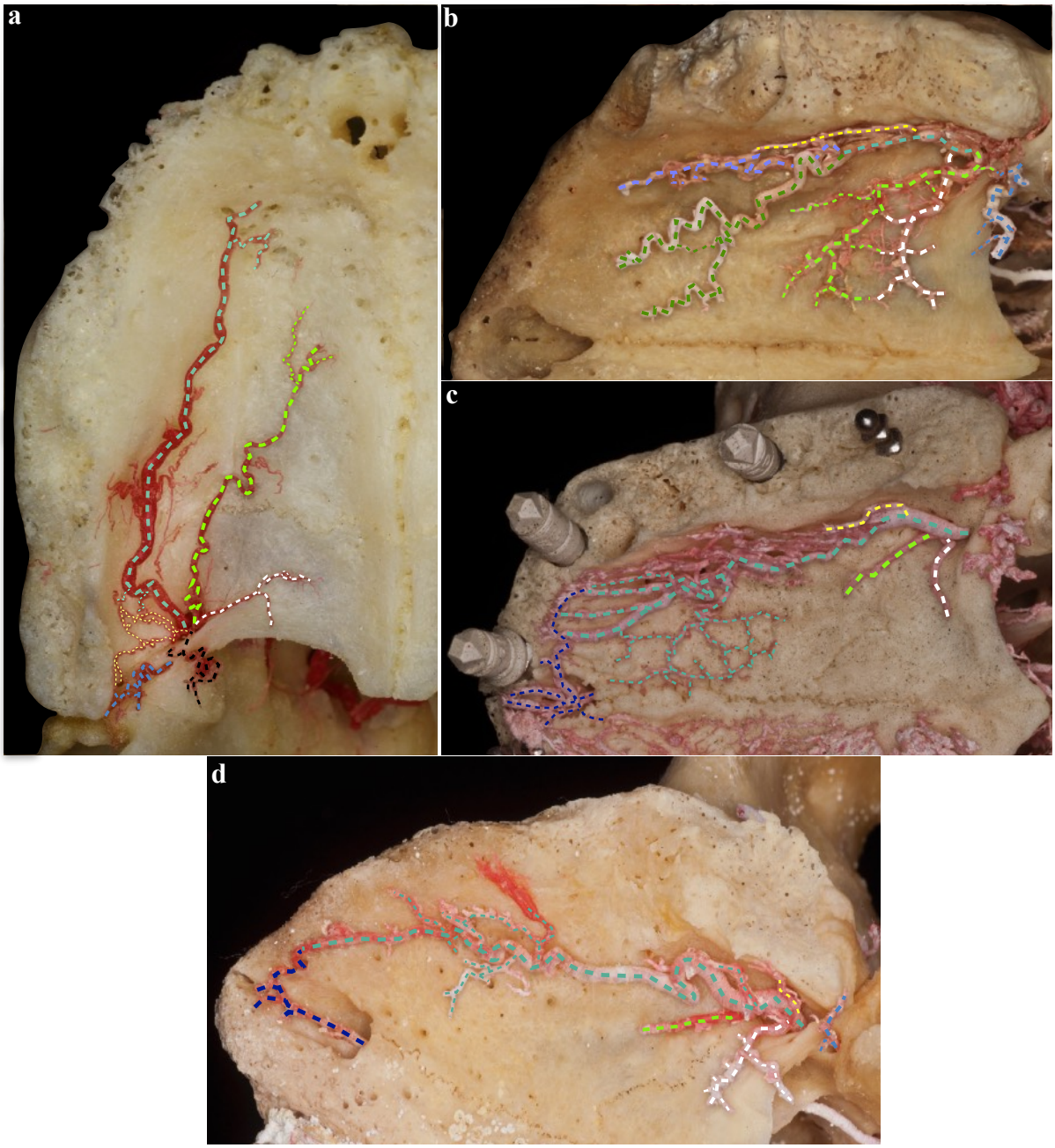

Fig. 11 Demonstration of the greater palatine artery (GPA) course and its main sub-branch variation by the corrosion casting method at the level of the greater palatine foramen and the premolar area. The lesser palatine artery (LPA) is observable in the pictures. **a)** GPA giving its sub-branches at the level of the greater palatine foramen supplying the maxillary tuberosity, the hard palate, the soft palate. **b)** The GPA divides to three main sub branches at the level of greater palatine foramen and premolar area. Ipsilateral anastomoses are visible. **c)** The GPA with 3 main branches at the level of greater palatine foramen and anastomosis with the nasopalatine artery (NPA). **d)** The GPA with 3 main branches at the level of greater palatine foramen and anastomosis with the ipsilateral vessels and the NPA.

DOI:10.14753/SE.2019.2327

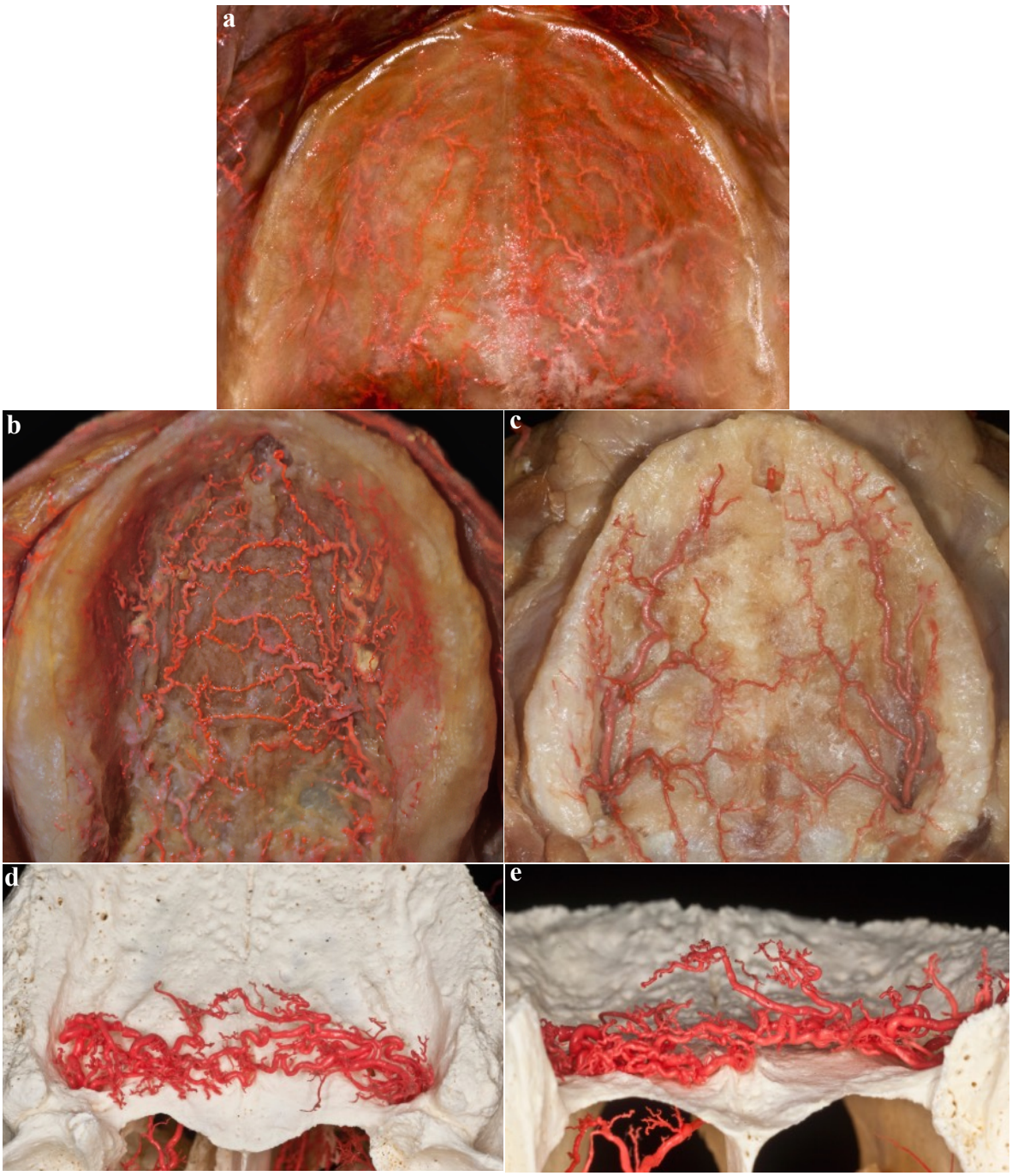

Fig. 12 Contralateral and ipsilateral anastomoses of the greater palatine artery (GPA) branches. **a)** Prior to dissection, just below the palatal mucosa, superficial ipsilateral and contralateral anastomoses were observed. **b)** The thin layer of mucosa was removed, and superficial contralateral anastomoses were detected. **c)** Deeper contralateral anastomoses at the level of the periosteum were found. **d)** Contralateral anastomoses stained by corrosion casting. **e)** Posterior view of contralateral anastomoses stained by corrosion casting.

DOI:10.14753/SE.2019.2327

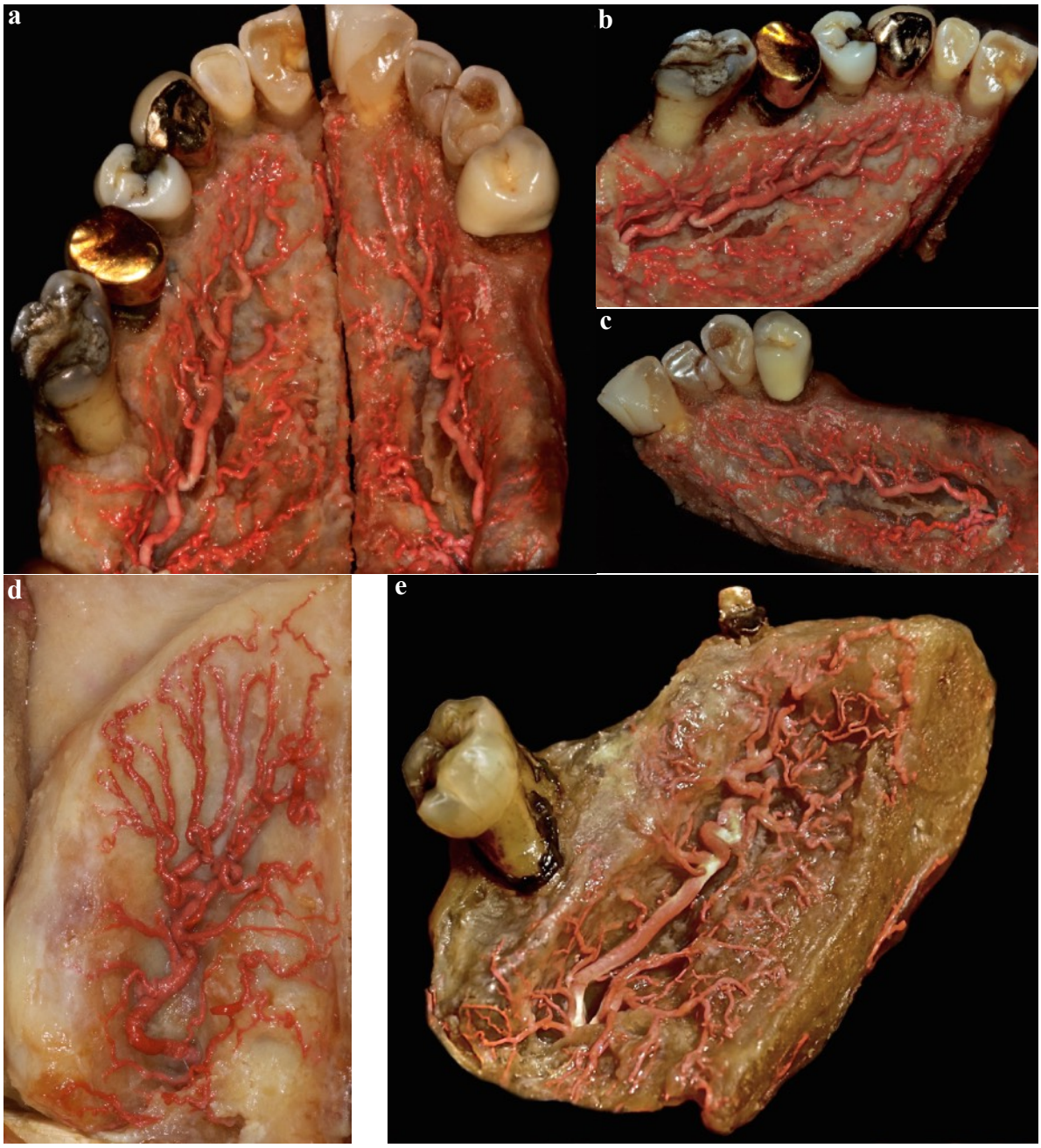

Fig. 13 Curvy pathway of the greater palatine artery (GPA) in the edentulous areas shown by latex milk injection. **a)** Bilateral view showing curvy pathway of the GPA, as well as horizontal shrinkage of the alveolar ridge due to atrophy at an edentulous site. **b)** Normal straight pathway of the GPA. **c)** Curvy pathway of the GPA at the area of the missing upper left molars. **d)** Excessively altered pathway of the GPA in a totally edentulous specimen. **e)** Curvy pathway of the GPA in the upper right premolar area.

DOI:10.14753/SE.2019.2327

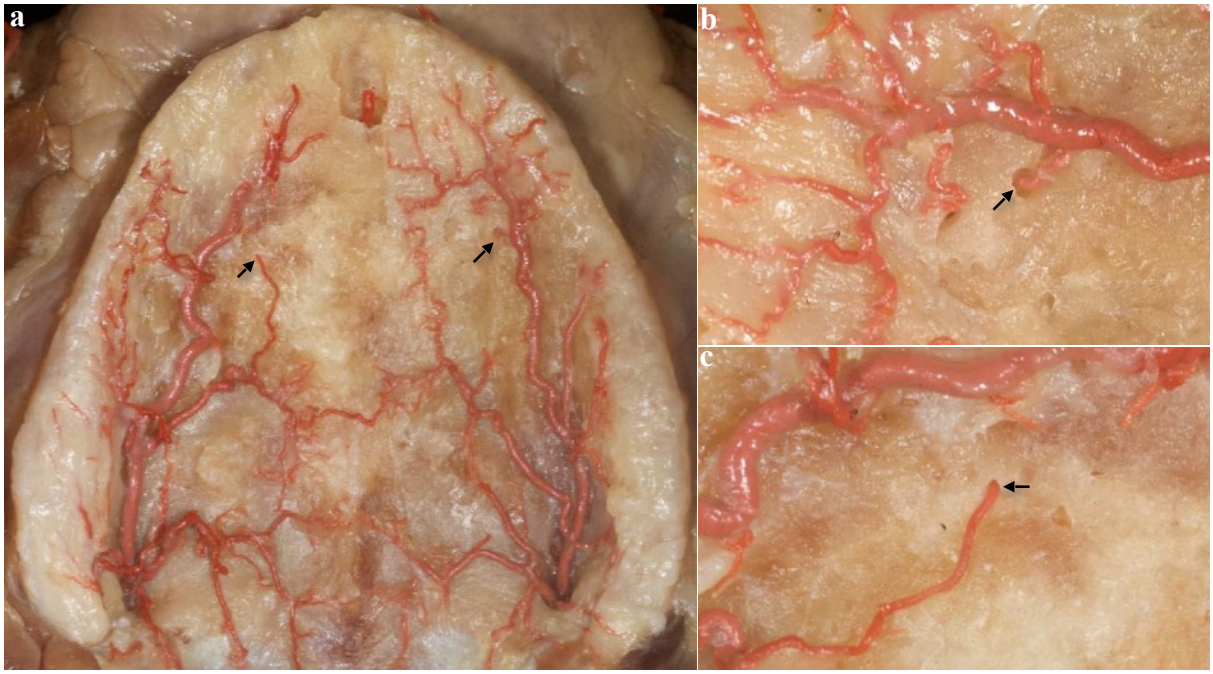

Fig. 14 Intraosseus branches of the greater palatine artery (GPA) shown by latex milk injection. **a)** Intraosseous arteries in the premolar area – bilateral overview. **b)** Intraosseous arteries in the premolar area – left side magnified view. **c)** Intraosseous branch penetrating the palatal cortical bone - right side magnified view.

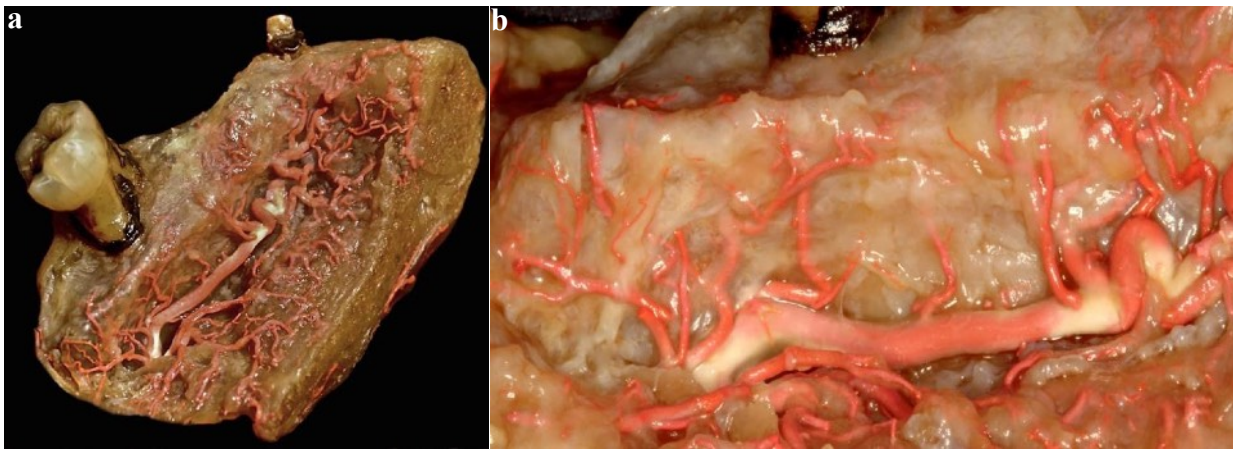

Fig. 15 Tuberal blood supply - Subbranches directly arise from the greater palatine artery (GPA). **a)** Overview, **b)** Magnified view.

DOI:10.14753/SE.2019.2327

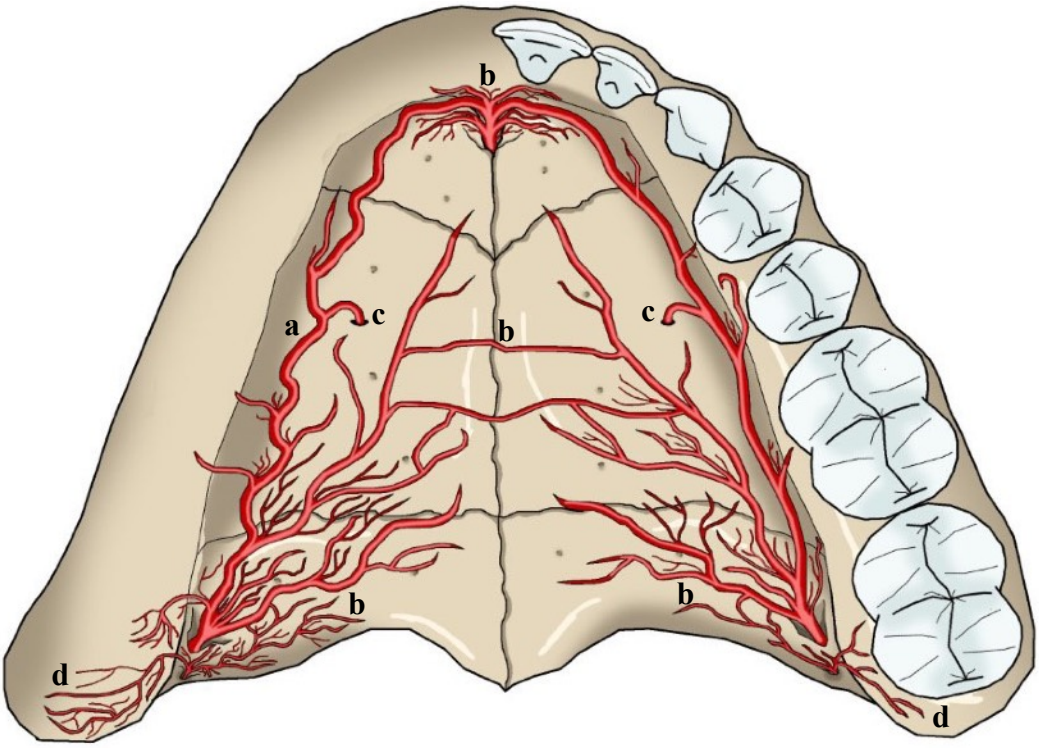

Fig. 16 Schematic drawing showing the complexity of the palatal blood supply.
a) Curvy greater palatine artery (GPA) pathway in the edentulous area due to the resorption of the bone compared to the dentate side. **b)** GPA anastomoses with the lesser palatine artery (LPA), nasopalatine artery (NPA) and contralateral GPA subbranches. **c)** Penetrating (intraosseous branches) in the premolar area. **d)** Tuberal blood supply by GPA and LPA sub-branches.

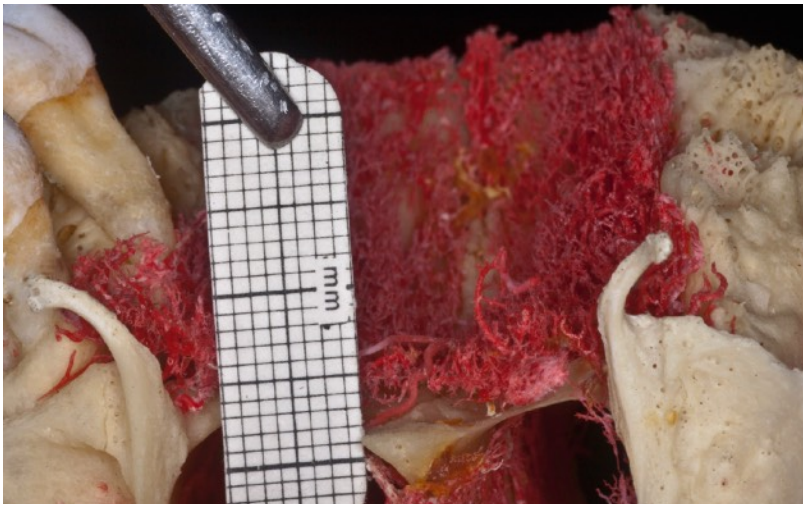

Fig. 17 Posterior view from the arterial network of the palate. At the level of 2nd molar the distance of greater palatine artery (GPA) from the gingival margin together with the thickness of the mucosal arterial supply was measured (~11.3 mm).

7. DISCUSSION

The results of our clinical and human cadaver studies allow us to discuss our findings with respect to the goals formulated in Chapter 4. The results of our studies have pointed to the important role and correlation of flap/incision design with angiogenesis, circulation, regeneration and periodontal wound healing.

In our clinical study, the split thickness flap was designed to eliminate damage to collateral vessels in patients presenting chronic periodontitis with localized three-dimensional alveolar defects. The horizonto-vertical alveolar reconstruction was carried out to optimize the crown:implant ratio, and to create favorable crestal bone levels, in line with adjacent periodontal tissues. Primary wound closure with proper blood supply was achieved and maintained during the complete period of healing in all three presented cases. GBR was performed in these patients by applying non-resorbable titanium membranes and the application of autogenous bone cylinders and particles, with or without the addition of BDX. This resulted in favorable hard tissue conditions around inserted implants regardless of the addition of BDX, which was confirmed by 9-month post-operative CBCT data, as well as direct clinical measurements during reentry. Optimal peri-implant soft tissue conditions were established in all reported cases; inserted implants were successfully loaded, and fulfilled the implant success criteria according to the International Congress of Oral Implantologists (Misch et al., 2008) during 5 years of follow-up.

Clinical results were comparable to available long term data reported after vertical augmentations (Simion et al., 2001). Follow-up radiographic findings supported the clinical observations, demonstrating 5 years of crystal bone stability without any clinically-significant remodeling around the inserted implants. The composite graft, a 1:1 mixture of particulate autogenous bone and xenograft materials, was used as a safe alternative in GBR procedures. This grafting approach has been well documented, and reported to be predictable and safe in the reconstruction of horizonto-vertical alveolar defects (Urban et al., 2009). Therefore, locally-harvested autogenous bone particles and minor tenting bone blocks combined with BDX were the grafting materials of choice in our case report.

The presented flap design is different from the surgical approach suggested by Tinti (1996) for augmentation procedures, which has been the standard protocol for vertical GBR during the last two decades, as confirmed by several different authors (Simion et al., 2007; Urban et al., 2015b). Vertical and horizontal releasing incisions, in combination with mucoperiosteal flaps, completely dissect the vascular architecture of the periosteal layer. In comparison to this full-thickness approach and previous split-thickness flap designs for ridge augmentation (Hur et al., 2010; Ogata et al., 2013), our novel, improved partial-thickness flap design was characterized by the following key elements: i) A split-thickness flap was elevated following mid-crestal incision, with a horizontal intracrevicular extension over two adjacent teeth. ii) Neither periosteal nor vertical releasing incisions were applied. iii) Ultimately, complete gap-free closure between the periosteal and lingual flaps was achieved by flap mobilization, this being the most significant attribute to allow for optimized postoperative blood supply (Windisch et al., 2017).

Two-layer wound closure resulted in improved flap revascularization during early wound healing, resulting in primary intention wound healing. Horizontal flap extension onto neighboring teeth, along with the split-thickness flap design, allowed additional tension-less handling and flap mobilization, compensating for the lack of vertical releasing incisions. The gap-free suturing of the intact periosteum with the mobilized oral flap withstood all kinds of muscular tension during the initial healing period and facilitated proper blood supply of the outer mucosal layer. Thus, membrane exposure due to muscle pull could be prevented in the early period of healing, resulting in primary wound closure in all reported cases. Soft tissue coverage was maintained throughout the whole healing period up to membrane removal in all cases, and no membrane exfoliations occurred.

Clinically-sufficient new hard tissue formation was observed at membrane removal in all cases. The need for bone harvesting could be minimized due to space maintenance provided by nonresorbable membranes and the tenting effect of micro-bone blocks. Thus, surgical interventions could be limited to one operation site. Newly-formed hard tissues resembling native bone were observed at membrane removal, regardless of the applied grafting material (autogenous bone and BDX in Case 1 and Case 3; autogenous

bone alone in Case 2). This indicated the significance of primary intention wound healing over non-resorbable membranes as an ultimate prerequisite for horizonto-vertical ridge reconstruction, provided by a predictable flap design and suturing approach. Direct clinical and radiographic measurements confirmed the complete fill of treated horizonto-vertical defects around the inserted implants.

In our case report, minor three-dimensional alveolar defects were treated around simultaneously-inserted dental implants. As a result of this, the mean measured vertical bone formation of 3.08 ± 1.25 mm was lower than that obtained in two-stage augmentation protocols reported previously (Simion et al., 1998; Simion et al., 2007; Urban et al., 2009) (Table 8). Significant remodeling of mucogingival conditions is a frequently-occurring phenomenon following bone grafting procedures, often requiring vestibuloplasty or widening of the peri-implant keratinized mucosa (Ueno et al., 2016). Such interventions were not needed in the presented cases, possibly due to lack of the vascular distortion usually originating from periosteal and vertical releasing incisions. Only a minor soft tissue augmentation was performed in Case 1 and Case 3: a subepithelial connective tissue graft was transplanted to ensure optimal peri-implant soft tissue thickness.

The proper width and thickness of keratinized tissues is of high clinical importance (Berglundh et al., 1991); this may have contributed to the long term stability of peri-implant soft and hard tissues observed during the 5-year follow-up after prosthetic loading. There are no relevant data referring to the success of vertical augmentation in patients with chronic periodontitis. All treated cases presented attachment loss and non-contained defect morphology in the close vicinity of the grafted area. These periodontal defects have been treated successfully, resulting in complete defect resolution (Table 7). This is well in line with the previous results reporting on simultaneous ridge augmentation and periodontal regeneration (Windisch et al., 2008).

According to the present results, reconstruction of localized, three-dimensional alveolar defects with a vertical component of 2 to 5 mm was demonstrated by applying the introduced novel partial-thickness flap design without periosteal or vertical releasing incisions, allowing for complete two-layer closure of soft tissues above the augmented

sites. The extent and duration of surgeries were minimized by utilizing a simultaneous approach and avoiding bone harvesting from donor sites. Thus, patient morbidity was kept within reasonable limits.

In oral and periodontal operations, a successful flap design, as presented in our first clinical study, results in anticipated wound healing, which is determined by undisturbed postoperative microcirculation, and preservation of tissues (Retzepi et al., 2007). The clinical success of our empirically-developed surgical approach and flap design led to further questions related to flap revascularization. Therefore we initiated a human cadaver study to gather more knowledge in this field. Our human cadaver findings, related to the vascular survey in the vestibule and palate, clearly allowed us to connect the gap between basic anatomical and empirical clinical knowledge, in order to understand the background of intra- and postoperative complications, as well as early wound healing events of palatal and vestibular surgical interventions.

A study by Kqiku et al. (2013) about the blood supply of the maxilla/maxillary sinus, investigated the extra- and intraosseous anastomoses between the PSAA (gingival and dental branches) and the IOA (extra- and intraosseous branches) and the mean distance between the anastomoses and the alveolar ridge. They measured the mean distance for the extraosseous anastomosis at the level of the upper second molar (16 mm), upper first molar (12.3 mm), upper second premolar (13.1 mm); and mean distance for the intraosseous anastomosis at the level of the upper second molar (17.7 mm), upper first molar (14.5 mm), upper second premolar (14.66 mm) (Kqiku et al., 2013). In our findings related to the blood supply of the upper oral vestibule in human cadavers, the orientation, direction and division of the PSAA, IOA and SLA with various superficial anastomoses were detected. Some of the anatomical characteristics were well in line with clinical observations related to post-surgical wound healing made in the daily practice. The anterior section of the upper vestibule did exhibit a typical straight orientation of arteries in the mucosal layer which were moving toward the interdental papillae and supplied the gingivae (Fig. 7, 8).

The paucity of dense vascular structures in the midbuccal areas implicates spoiled blood circulation. This confirms the observation of inept consequences (scars, gingival recessions) if vertical releasing incisions are designed at the midline gingival zenith of front teeth. In the posterior dentate maxilla, according to the transverse path of significant branches in the mucosa (Fig. 8), vertical releasing incisions might disturb the circulation between distal and mesial tissues. In the lower vestibule, the critical location of the ILA was observed. The horizontal course of this artery became superficial together with the vertical branches moving toward the papillae. Also higher density of superficial blood vessels were found in the mucosa at the level of the molars (Fig. 9). By these novel findings, any vertical incision in the lower vestibule between the first molar and second premolars might be avoided to prevent from intra- and postoperative complications, and reduce the risk of injury to the circulation of arterial network.

With our palatal vascular distribution study, we were able to present comprehensive novel results related to palatal blood supply, which can be integrated into clinical practice when planning and executing palatal surgical interventions. Information available in anatomical literature and textbooks lacks clinically-focused details of the palatal vascular network (intraosseous branches; various anastomoses, affecting the injection of local anesthetics and incision design; changes in the course of vascular pathways due to loss of dentition and bone resorption). Our study provided a solid anatomical basis describing local characteristics of the hard palate and maxillary tuberosity for clinicians who are interested in surgical interventions of the posterior maxilla, such as connective tissue grafting, removal of impacted canines, implant placement and sinus floor elevation. We demonstrated the course and arterial anastomoses between contralateral and ipsilateral vessels of the palate (Fig. 10, 11,12) along with additional vascular mapping of the maxillary tuberosity (Fig. 15). The application of corrosion casting and latex milk injection following Thiel's fixation simultaneously allowed for blood vessel mapping together with localization of arteries within the palatal mucosa relative to already identified anatomical landmarks. This unique combination of different staining methods has enabled us to demonstrate new types of anastomoses between the GPA, NPA and LPA, or previously unknown

intraosseous branches of the GPA, alteration of the GPA pathway in edentulous sites and tuberal blood supply (Shahbazi et al., 2018).

Corrosion casting is a widely-recognized method in the literature for the three dimensional visualization of vascular structures (Verli et al., 2007; Haenssgen et al., 2014). In the present study, this approach was successfully applied to investigate possible previously unknown pathways of the GPA and its sub-branches. Moreover, we utilized latex milk injection (Alvernia et al., 2010) to visualize the topographical relation of the GPA branches and sub-branches to adjacent tissues within the palatal masticatory mucosa. The palatal mucosa is the most frequently-used donor site for connective tissue graft harvesting (Zuhr et al., 2014). Nevertheless, there is only scarce data on the palatal anastomoses that possibly influence intraoperative bleeding and postoperative blood supply of palatal donor sites. SCTGs are usually harvested from an area between the canine and the second molar of the palate by leading a horizontal incision, and the tissue is then harvested by either the trapdoor technique (Cortellini et al., 1995) or the single incision approach (Hürzeler & Weng, 1999). These approaches, depending on the number, direction and depth of incisions, might produce a certain risk for arterial damage and a compromised postoperative blood supply. According to our results, several cases of contra- and ipsilateral anastomoses between the GPA, NPA and LPA were demonstrated in the cadavers studied. This might provide an anatomical basis for physiological experiments investigating whether additional submucosal deposition of local anesthetics to contralateral major palatal foramen and/or nasopalatal foramen might be necessary to reduce intraoperative bleeding during palatal surgeries, e.g. SCTG harvesting and sinus floor elevation. Moreover, based on the presence of newly-found contralateral anastomoses, we think that in surgeries concerning the palate, contralateral blood circulation might also be affected. Therefore, bilateral connective tissue harvesting may lead to impaired postoperative blood supply and flap necrosis.

We also successfully demonstrated the existence of the intraosseous GPA branches of palatal arteries, which have not been documented previously (Fig. 14). A similar anatomical relation is known in the lower jaw, where nutritive sub-branches of the sublingual arteries penetrate the lingual cortical layer of the mandible (Liang et al., 2007; He et al., 2017). Based on anatomical and clinical experiences with lingual

intraosseous arteries (He et al., 2017), their palatal counterparts might be responsible for the nutrition of the maxilla and possibly the Schneiderian membrane. Nevertheless, due to their small diameter, they do not pose a significant risk for profuse intraoperative bleeding when compared to lingual nutritive branches. The distribution of the palatal intraosseous branches showed a pattern running parallel to the pathway of the GPA.

A study by Reiser et al. (1996) suggested that the greater palatine nerves and vessels lie 17 mm from the gingival margin in high palatal (U shaped) vault, 12 mm from the gingival margin in medium palatal vault, while in low palatal (flat) vault the distance was 7 mm. According to our present findings in edentulous cadavers, due to the resorption of the alveolar ridge, the area for the pathway of the GPA might decrease in apico-coronal and oro-vestibular dimensions, and the GPA would exhibit a more undulating pathway. We were able to demonstrate that, in edentulous cases, the GPA and its sub-branches became more superficial, which might increase the risk of GPA injury during any type of palatal flap preparation, e.g. connective tissue graft harvesting or during augmentation procedures. Due to this specific curvy outline of arteries, the distance of the GPA from the crest was reduced by 3-4 mm, thus increasing the risk for arterial injury during connective tissue harvesting (Fig. 13). Therefore, at edentulous sites, superficial removal of a FGG can be a more secure clinical procedure for connective tissue harvesting, as opposed to the single incision or trapdoor techniques. Apart from the detailed description of the palatal arterial pathways, we were also able to visualize the blood supply of the maxillary tuberosity. The GPA and LPA send one or two minor branches here, which provide for the nutrition of this area. The tuberosity is considered as a possible alternative for the hard palate for SCTG or FGG harvesting when applying the distal wedge procedure (Robinson, 1966). The fact that the GPA and LPA branches directed towards the tuberosity are significantly smaller and have lower density compared to palatal arteries might be the reason for prolonged graft revascularization and incorporation, and this is likely to be associated with frequent partial or total necrosis of tuberal FGGs.

DOI:10.14753/SE.2019.2327

8. CONCLUSION

In this section the major conclusions from clinical and human cadaver investigations will be drawn. The following statements are related to a clinical case report study (I), and human cadaver research providing the methodological basis for future modeling of novel flap designs for graft harvesting and reconstructive procedures (II).

Study I

The presented two-layer split-thickness flap without damaging of collateral vessels, combined with the GBR technique utilizing titanium membranes, autologous and xenograft materials resulted in a predictable three-dimensional reconstruction of hard tissues. The reconstructed peri-implant hard tissues showed excellent stability up to 5 years after functional loading. The newly-introduced surgical approach can be utilized for the localized horizonto-vertical reconstruction of edentulous alveolar ridges and adjacent periodontal defects along with simultaneous implant placement.

Study II

a) The vascular survey findings of the oral vestibule represent a sound anatomical background for currently used split thickness surgical techniques performed in the vestibule for reconstructive surgical interventions. By the latex milk injection, the orientation (vertical or transverse), division and anastomoses of the vessels were demonstrated. This might help clinicians designing novel surgical approaches aimed at reducing postoperative wound healing complications.
b) In the palatal vascular distribution study, corrosion casting and latex milk injection methods were successfully applied to investigate the pathways of the GPA, NPA and LPA and their sub-branches with their complex network of the anastomoses. Previously unknown intraosseous branches of the GPA were detected. Furthermore, we were able to study the curved alteration of GPA pathways in edentulous sites and the tuberal blood supply.

The combination of clinical and anatomical findings have shed light on findings with relevance to vestibular and palatal blood supply, offering a powerful tool for the design and execution of surgical interventions involving the hard palate and oral vestibule.

DOI:10.14753/SE.2019.2327

9. SUMMARY

Several flaps/incisions techniques have been suggested in the past for reconstructive and graft harvesting procedures. Based on our clinical case report study (I) in the vestibule, a novel split-thickness flap design without periosteal and vertical releasing incisions for horizonto-vertical ridge augmentation is suggested. By this method, the collateral vessels are protected and as a result, proper angiogenesis combined with wound healing were achieved. In all three cases, the GBR technique utilizing titanium membranes in combination with autologous and xenogeneic grafting materials applied with the presented split-thickness flap resulted in predictable hard tissue reconstruction.
In human cadaver study (II), a detailed macroscopic vascular mapping of the oral vestibule, hard palate and maxillary tuberosity together with their anastomoses were detected. The pathway of the vessels with their anastomoses were stained by the latex milk injection and corrosion casting methods.

In study II/a, the course of major and sub-branches of the SLA, IOA, PSAA and ILA with their different anastomoses were recorded by the latex milk injection technique in the upper and lower vestibules, in ten head specimens. This method has revealed findings with relevance to the vestibular blood supply, offering a powerful tool for flap design and execution of surgical interventions involving the vestibule.

In study II/b, a detailed macroscopic analysis of the palatal and tuberal vascular supply together with their anastomoses were recorded in ten cadavers. The vessels were stained by the corrosion casting and latex milk injection methods. The major- and secondary branches of the GPA and it's relation to the palatine spine and various anastomoses were demonstrated. Penetrating intraosseous branches at the premolar-canine area were also detected. In edentulous patients the GPA developed a curvy pathway in the premolar area.

These studies might provide clinicians with solid clinical and anatomical knowledge to understand the structural background of blood vessel distribution influencing intra- and postoperative complications, as well as early wound healing events of vestibular and palatal surgical interventions with less invasive and optimized flap designs.

DOI:10.14753/SE.2019.2327

10. ÖSSZEFOGLALÁS

Az irodalomban számos lebenytechnikát írtak le kemény- és lágyszöveti rekonstruktív parodontális és dentoalveoláris sebészeti és graftkivételi technikákhoz. Klinikai vizsgálatunk (I) alapján egy újszerű - vertikális segédmetszéseket és perioszteális metszéseket nem alkalmazó - félvastag lebeny alkalmazása javasolt nagy kiterjedésű alveoláris gerinchiányok rekonstrukciójára. Ennél a technikánál a kollaterális keringés nem károsodik, és így biztosított a megfelelő posztoperatív angiogenezis és a zavartalan sebgyógyulás. Félvastag lebeny és feltárásból, titán membránnal és kompozit grafttal (50% autogén csontforgács - 50% bovin eredetű xenograft) végzett GBR mindhárom esetben kiszámítható keményszöveti regenerációt eredményezett. Egy humán kadáver vizsgálat (II) során, részletesen feltérképeztük a vesztibulum, a kemény szájpad és a tuber maxillae vérellátását és a közöttük fellelhető anasztomózisokat. Az erek lefutását latex tej befecskendezéssel és korróziós kiöntéssel tettük láthatóvá a kadávereken. A vizsgálat anatómiai alapismereteket nyújt a gyakorló klinikus számára, hogy a terület vérellátásának pontos ismerete birtokában elkerülhesse az esetleges intra- és posztoperatív komplikációkat.

A II/a vizsgálatban az a. labialis superior, a. infraorbitalis, a. alveolaris superior posterior és az a. labialis inferior fő- és mellékágainak lefutását és ansztomózisait vizsgáltuk latex tej befecskendezés segítségével a felső és az alsó vesztibulumban, tíz preparátumon. Megfigyeléseink a sebészeti beavatkozások alkalmával segítséget nyújtanak a gyakorló orvosok számára lebenyképzés során.

A II/b vizsgálat során tíz preparátumon mutattuk be a palatum és a tuber maxillae vérellátásának makroszkópos struktúráját. Az a. palatinus majus fő- és mellékágainak lefutását és az a. nasopalatinus-szal és az a. palatinus minus-szal képzett anasztomózisait szemléltettük. A szemfog és a premoláris fogak magasságában az a. palatinus majus egyes ágai átfúrják a csontot és intraosszeálisan haladnak tovább. Fogatlan páciensek esetén az a. palatinus majus lefutása kanyargósabbá válik.

Ezek a vizsgálatok támpontot nyújtanak a gyakorló fogorvosok számára a műtétek tervezésénél és az intra- és posztoperatív komplikációk elkerülésénél.

11. BILBIOGRAPHY

1. Abrams H, Gossett SE, Morgan WJ. (1988) A modified flap design in exposing the palatally impacted canine. ASDC J Dent Child, 55:285-287.

2. Alvernia JE, Pradilla G, Mertens P, Lanzino G, Tamargo RJ. (2010) Latex injection of cadaver heads: technical note. Neurosurgery, 67 (2 Suppl Operative): 362-367.

3. Arnold F, West DC. (1991) Angiogenesis in wound healing. Pharmacol Ther, 52:407-422.

4. Benninger B, Andrews K, Carter W. (2012) Clinical measurements of hard palate and implications for subepithelial connective tissue grafts with suggestions for palatal nomenclature. J Oral Maxillofac Surg, 70:149-153.

5. Bergeron L, Tang M, Morris SF. (2006) A review of vascular injection techniques for the study of perforator flaps. Plast Reconstr Surg, 117:2050-2057.

6. Berglundh T, Lindhe J, Ericsson I, Marinello CP, Liljenberg B, Thomsen P. (1991) The soft tissue barrier at implants and teeth. Clin Oral Implants Res, 2:81-90.

7. Berkovitz BKB, Holland GR, Moxham BJ. Oral Anatomy, Histology and Embryology (4th ed.). MOSBY/ELSEVIER, Edinburgh, 2009:2-4.

8. Buser D, Chappuis V, Kuchler U, Bornstein MM, Wittneben JG, Buser R, Cavusoglu Y, Belser UC. (2013) Long-term stability of early implant placement with contour augmentation. J Dent Res, 92(12_suppl), 176S-182S.

9. Buser D, Halbritter S, Hart C, Bornstein MM, Grütter L, Chappuis V, Belser UC. (2009) Early implant placement with simultaneous guided bone regeneration following single-tooth extraction in the esthetic zone: 12-month results of a prospective study with 20 consecutive patients. J Periodontol, 80: 152-162.

10. Choi J, Park HS. (2003) The clinical anatomy of the maxillary artery in the pterygopalatine fossa. J Oral Maxillofac Surg, 61:72-78.

11. Chrcanovic BR, Custódio AL. (2010) Anatomical variation in the position of the greater palatine foramen. J Oral Sci, 52:109-113.

12. Cortellini P, Pini-Prato G, Tonetti MS. (1995) Interproximal free gingival grafts after membrane removal in guided tissue regeneration treatment of intrabony defects. A randomized controlled clinical trial. J Periodontol, 66:488-493.

13. Cortellini P, Tonetti MS. (2015) Clinical concepts for regenerative therapy in intrabony defects. Periodontol 2000, 68:282-307.

14. Donos N, Mardas N, Chadha V. (2008) Clinical outcomes of implants following lateral bone augmentation: systematic assessment of available options (barrier membranes, bone grafts, split osteotomy). J Clin Periodontol, 35 (8 Suppl): 173-202.

15. Echt A. Rubber tree cultivation. In: Stellman JM (Ed.), *Encyclopaedia of Occupational Health and Safety* (4th ed., Vol. 3). International Labour Office, Geneva, 1998:80.3-80.4.

16. Edel A. (1974) Clinical evaluation of free connective tissue grafts used to increase the width of keratinised gingiva. J Clin Periodontol, 1:185-196.

17. Egelberg J. (1966) The blood vessels of the dentogingival junction. J Periodontal Res, 1:163-179.

18. Fickl S, Kebschull M, Schupbach P, Zuhr O, Schlagenhauf U, Hürzeler MB. (2011) Bone loss after full-thickness and partial-thickness flap elevation. J Clin Periodontol, 38:157-162.

19. Fu JH, Hasso DG, Yeh CY, Leong DJ, Chan HL, Wang HL. (2011) The accuracy of identifying the greater palatine neurovascular bundle: a cadaver study, J Periodontol, 82:1000-1006.

20. Gray H, Lewis WH. Anatomy of the Human Body (20th ed.). Lea & Febiger, Philadelphia, 1918:1110-1112.

21. Graziani F, Karapetsa D, Mardas N, Leow N, Donos N. (2018) Surgical treatment of the residual periodontal pocket. Periodontol 2000, 76:150-163.

22. Griffin TJ, Cheung WS, Zavras AI, Damoulis PD. (2006) Postoperative complications following gingival augmentation procedures. J Periodontol, 77:2070-2079.

23. Haenssgen K., Makanya A. N., Djonov V. (2014) Casting Materials and their Application in Research and Teaching. Microsc Microanal, 20:493-513.

24. Han TJ, Klokkevold PR, Takei HH. (1995) Strip gingival autograft used to correct mucogingival problems around implants. Int J Periodontics Restorative Dent, 15:404-411.

25. Harris RJ, Miller R, Miller LH, Harris C. (2005) Complications with surgical procedures utilizing connective tissue grafts: a follow-up of 500 consecutively treated cases. Int J Periodontics Restorative Dent, 25:449-459.

26. He P, Truong MK, Adeeb N, Tubbs RS, Iwanaga J. (2017) Clinical anatomy and surgical significance of the lingual foramina and their canals, Clin Anat, 30:194-204.

27. Hill EG Jr, McKinney WM. (1981) Vascular anatomy and pathology of the head and neck: method of corrosion casting. Adv Neurol, 30:191-197.

28. Hoke JA, Burkes EJ, White JT, Duffy MB, Klitzman B. (1994) Blood-flow mapping of oral tissues by laser Doppler flowmetry. Int J Oral Maxillofac Surg, 23:312-315.

29. Hodde KC, Steeber DA, Albrecht RM. (1990) Advances in corrosion casting methods. Scanning Microsc, 4:693-704.

30. Hossler FE, Douglas JE. (2001) Vascular Corrosion Casting: Review of Advantages and Limitations in the Application of Some Simple Quantitative Methods. Microsc Microanal, 7:253-264.

31. Hur Y, Tsukiyama T, Yoon TH, Griffin T. (2010) Double flap incision design for guided bone regeneration: a novel technique and clinical considerations. J Periodontol, 81:945-952.

32. Hürzeler MB, Weng D. (1999) A single-incision technique to harvest subepithelial connective tissue grafts from the palate. Int J Periodontics Restorative Dent, 19:279-287.

33. Kim DH, Won SY, Bae JH, Jung UW, Park DS, Kim HJ, Hu KS. (2014) Topography of the greater palatine artery and the palatal vault for various types of periodontal plastic surgery. Clin Anat, 27:578–584.

34. Kishi Y, Takahashi K, Trowbridge H. (1990) Vascular network in papillae of dog oral mucosa using corrosive resin casts with scanning electron microscopy. Anat Rec, 226:447-459.

35. Kleinheinz J, Büchter A, Kruse-Lösler B, Weingart D, Joos U. (2005) Incision design in implant dentistry based on vascularization of the mucosa. Clin Oral Implants Res, 16:518-523.

36. Klosek SK, Rungruang T. (2009) Anatomical study of the greater palatine artery and related structures of the palatal vault: considerations for palate as the subepithelial connective tissue graft donor site. Surg Radiol Anat, 31:245-250.

37. Koymen R, Karacayli U, Gocmen-Mas N, Ertugrul-Koymen C, Ortakoglu K, Gunaydin Y, Magden O. (2009) Flap and incision design in implant surgery: clinical and anatomical study. Surg Radiol Anat, 31:301-306.

38. Köşger H, Polat HB, Demirer S, Ozdemir H, Ay S. (2009) Periodontal healing of marginal flap versus paramarginal flap in palatally impacted canine surgery: a prospective study. J Oral Maxillofac Surg, 67:1826-1831.

39. Kqiku L, Biblekaj R, Weiglein AH, Kqiku X, Städtler P. (2013) Arterial blood architecture of the maxillary sinus in dentate specimens. Croat Med J, 54:180-184.

40. Lametschwandtner A, Lametschwandtner U, Weiger T. (1990) Scanning electron microscopy of vascular corrosion casts-technique and applications: updated review. Scanning Microsc, 4:889-940.

41. Langer B, Calagna L. (1980) The subepithelial connective tissue graft. J Prosthet Dent, 44:363-367.

42. Langer B, Langer L. (1985) Subepithelial connective tissue graft technique for root coverage. J Periodontol, 56:715-720.

43. Langer L, Langer B. (1993) The subepithelial connective tissue graft for treatment of gingival recession. Dent Clin North Am, 37:243-264.

44. Liang X, Jacobs R, Lambrichts I, Vandewalle G. (2007) Lingual foramina on the mandibular midline revisited: a macroanatomical study, Clin Anat, 20:246-251.

45. Lim G, Lin GH, Monje A, Chan HL, Wang HL. (2018) Wound Healing Complications Following Guided Bone Regeneration for Ridge Augmentation: A Systematic Review and Meta-Analysis. Int J Oral Maxillofac Implants, 33:41-50.

46. Lindhe J, Karring T, Araújo M. Anatomy of periodontal tissues. In: Lindhe J, Lang NP (Eds.), *Clinical Periodontology and Implant Dentistry* (6th ed., Vol.1). Wiley Blackwell, Chichester, 2015:3-46.

47. Misch CE, Perel ML, Wang HL, Sammartino G, Galindo-Moreno P, Trisi P, Steigmann M, Rebaudi A, Palti A, Pikos MA, Schwartz-Arad D, Choukroun J, Gutierrez-Perez JL, Marenzi G, Valavanis DK. (2008) Implant success, survival, and failure: the International Congress of Oral Implantologists (ICOI) Pisa Consensus Conference. Implant Dent,17:5-15.

48. Molnár E, Molnár B, Lohinai Z, Tóth Z, Benyó Z, Hricisák L, Windisch P, Vág J. (2017) Evaluation of laser speckle contrast imaging for the assessment of oral mucosal blood flow following periodontal plastic surgery: an exploratory study. Biomed Res Int, 2017:4042902.

49. Mörmann W, Ciancio SG. (1977) Blood supply of human gingiva following periodontal surgery. A fluorescein angiographic study. J Periodontol, 48:681-692.

50. Motoyama AA, Watanabe IS. (2001) Light and scanning electron microscopic studies of the angioarchitecture of intrinsic muscle fibers of the anterior rat tongue. J Oral Sci, 43:269-275.

51. Niu L, Wang J, Yu H, Qiu L. (2018) New classification of maxillary sinus contours and its relation to sinus floor elevation surgery. Clin Implant Dent Relat Res, 20:493-500.

52. Ogata Y, Griffin TJ, Ko AC, Hur Y. (2013) Comparison of double-flap incision to periosteal releasing incision for flap advancement: a prospective clinical trial. Int J Oral Maxillofac Implants, 28:597-604.

53. Oh SL, Masri RM, Williams DA, Ji C, Romberg E. (2017) Free gingival grafts for implants exhibiting lack of keratinized mucosa: a prospective controlled randomized clinical study. J Clin Periodontol, 44:195-203.

54. Ojima K, Saiki C, Takahashi T, Matsumoto S, Takeda M. (1997) Angioarchitectural structure of the fungiform papillae on the anterodorsal surface of the rat tongue. Ann Anat, 179, 399-403.

55. Ottone NE, Vargas CA, Fuentes R, Del Sol M. (2016) Walter Thiel's Embalming Method. Review of Solutions and Applications in Different Fields of Biomedical Research. Int. J. Morphol, 34:1442-1454.

56. Pilsl U, Anderhuber F, Neugebauer S. (2016) The Facial Artery-The Main Blood Vessel for the Anterior Face? Dermatol Surg, 42:203-208.

57. Polimeni G, Xiropaidis AV, Wikesjö Ulf ME. (2006) Biology and principles of periodontal wound healing/regeneration. Periodontol 2000, 41:30-47.

58. Rahpeyma A, Khajehahmadi S. (2017) Maxillary artery based flaps for oral cavity reconstruction, a review. Ann Med Surg (Lond), 20:32-36.

59. Reiser GM, Bruno JF, Mahan PE, Larkin LH. (1996) The subepithelial connective tissue graft palatal donor site: anatomic considerations for surgeons. Int J Periodontics Restorative Dent, 16:130-137.

60. Retzepi M, Tonetti M, Donos N. (2007) Gingival blood flow changes following periodontal access flap surgery using laser Doppler flowmetry. J Clin Periodontol, 34:437-443.

61. Rueda Esteban RJ, López McCormick JS, Martínez Prieto DR, Hernández Restrepo JD. (2017) Corrosion Casting, a Known Technique for the Study and Teaching of Vascular and Duct Structure in Anatomy. Int. J. Morphol, 35:1147-1153.

62. Robinson RE. (1966) The distal wedge operation. Periodontics, 4:256-264.

63. Selliseth NJ, Selvig KA. (1993) Microvasculature of the dorsum of the rat tongue: a scanning electron microscopic study using corrosion casts. Scand J Dent Res, 101: 391-397.

64. Selliseth NJ, Selvig KA. (1995) Revascularization of an excisional wound in gingiva and oral mucosa. A scanning electron microscopic study using corrosion casts in rats. Scanning Microsc, 9:455-467.

65. Shahbazi A, Grimm A, Feigl G, Gerber G, Székely AD, Molnár B, Windisch P. (2018) Analysis of blood supply in the hard palate and maxillary tuberosity — clinical implications for flap design and soft tissue graft harvesting (a human cadaver study). Clin Oral Invest, 23:1153-1160.

66. Simion M, Fontana F, Rasperini G, Maiorana C. (2004) Long-term evaluation of osseointegrated implants placed in sites augmented with sinus floor elevation associated with vertical ridge augmentation: a retrospective study of 38 consecutive implants with 1- to 7- year follow-up. Int J Periodontics Restorative Dent, 24:208-221.

67. Simion M, Fontana F, Rasperini G, Maiorana C. (2007) Vertical ridge augmentation by expanded-polytetrafluoroethylene membrane and a combination of intraoral autogenous bone graft and deproteinized anorganic bovine bone (Bio Oss). Clin Oral Implants Res, 18:620-629.

68. Simion M, Jovanovic SA, Tinti C, Benfenati SP. (2001) Long-term evaluation of osseointegrated implants inserted at the time or after vertical ridge augmentation. A retrospective study on 123 implants with 1-5 year follow-up. Clin Oral Implants Res, 12:35-45.

69. Simion M, Jovanovic SA, Trisi P, Scarano A, Piattelli A. (1998) Vertical ridge augmentation around dental implants using a membrane technique and autogenous bone or allografts in humans. Int J Periodontics Restorative Dent, 18:8-23.

70. Sims PA, Albrecht RM. (1993) Improved tissue corrosion of vascular casts: a quantitative filtration method used to compare tissue corrosion in various concentrations of sodium and potassium hydroxide. Scanning Microsc, 7:637-642.

71. Sullivan HC, Atkins JH. (1969) The role of free gingival grafts in periodontal therapy. Dent Clin North Am, 13:133-148.

72. Thiel W. (1992a) The preservation of whole corpse with natural color. Ann Anat, 174:185-195.

73. Thiel W. (1992b) Eine Arterienmasse zur Nachinjektion bei der konservierung ganzer Leichen. Ann Anat, 174:197-200.

74. Thiel W. (2002) Ergänzung für die Konservierung ganzer Leichen nach W. Thiel. Ann Anat, 184:267-269.

75. Tinti C, Parma-Benfenati S, Polizzi G. (1996) Vertical ridge augmentation: what is the limit? Int J Periodontics Restorative Dent, 16:220-229.

76. Ueno D, Nagano T, Watanabe T, Shirakawa S, Yashima A, Gomi K. (2016) Effect of the Keratinized Mucosa Width on the Health Status of Periimplant and Contralateral Periodontal Tissues: A Cross-sectional Study. Implant Dent, 25:796-801.

77. Urban IA, Jovanovic SA, Lozada JL. (2009) Vertical ridge augmentation using guided bone regeneration (GBR) in three clinical scenarios prior to implant placement: a retrospective study of 35 patients 12 to 72 months after loading. Int J Oral Maxillofac Implants, 24:502-510.

78. Urban IA, Lozada JL, Nagy K, Sanz M. (2015a) Treatment of severe mucogingival defects with a combination of strip gingival grafts and a xenogeneic collagen matrix: a prospective case series study. Int J Periodontics Restorative Dent, 35:345-353.

79. Urban IA, Monje A, Wang HL. (2015b) Vertical Ridge Augmentation and Soft Tissue Reconstruction of the Anterior Atrophic Maxillae: A Case Series. Int J Periodontics Restorative Dent, 35:613-623.

80. Verli FD, Kraether Neto L, Cherubini K, Souza MAL. (2006) A technical approach of vascular corrosion casts in odontological research. RFO UPF, 11: 7-12.

81. Verli FD, Rossi-Schneider TR, Schneider FL, Yurgel LS, De Souza MAL. (2007) Vascular Corrosion Casting Technique Steps. Scanning, 29:128-132.

82. Wang HL, Al-Shammari K. (2002) HVC ridge deficiency classification: a therapeutically oriented classification. Int J Periodontics Restorative Dent, 22:335-343.

83. Windisch P, Martin A, Shahbazi A, Molnar B. (2017) Reconstruction of horizontovertical alveolar defects. Presentation of a novel split-thickness flap design for guided bone regeneration: A case report with 5-year follow-up. Quintessence Int, 48:535-547.

84. Windisch P, Szendroi-Kiss D, Horváth A, Suba Z, Gera I, Sculean A. (2008) Reconstructive periodontal therapy with simultaneous ridge augmentation. A clinical and histological case series report. Clin Oral Investig, 12:257-264.

85. Yu SK, Lee MH, Park BS, Jeon YH, Chung YY, Kim HJ. (2014) Topographical relationship of the greater palatine artery and the palatal spine. Significance for periodontal surgery. J Clin Periodontol, 41:908-913.

86. Zucchelli G, De Sanctis M. (2000) Treatment of multiple recession-type defects in patients with esthetic demands. J Periodontol, 71:1506-1514.

87. Zucchelli G, Testori T, De Sanctis M. (2006) Clinical and anatomical factors limiting treatment outcomes of gingival recession: a new method to predetermine the line of root coverage. J Periodontol, 77: 714-721.

88. Zuhr O, Bäumer D, Hürzeler M. (2014) The addition of soft tissue replacement grafts in plastic periodontal and implant surgery: critical elements in design and execution. J Clin Periodontol, 15: S123-S142.

12. BIBLIOGRAPHY OF THE CANDIDATE'S PUBLICATIONS

- **Related publications**

(I) Windisch P, Martin A, **Shahbazi A**, Molnar B. (2017). Reconstruction of horizontovertical alveolar defects. Presentation of a novel split-thickness flap design for guided bone regeneration: A case report with 5-year follow-up. Quintessence Int. 48(7):535-547. doi: 10.3290/j.qi.a38354. ***IF: 1.088***

(II) Arvin Shahbazi, András Grimm, Georg Feigl, Gábor Gerber, Andrea Dorottya Székely, Bálint Molnár, Péter Windisch. (2018). Analysis of blood supply in the hard palate and maxillary tuberosity — clinical implications for flap design and soft tissue graft harvesting (a human cadaver study). Clin Oral Investig. 23(3):1153-1160. doi: 10.1007/s00784-018-2538-3. ***IF: 2.386***

13. ACKNOWLEDGEMENTS

- **Study I**

The study was made at the Department of Periodontology, Semmelweis University, Budapest, Hungary.

- **Study II**

The study was made at the Department of Periodontology, Semmelweis University, and the Department of Anatomy, Histology and Embryology, Semmelweis University, Budapest, Hungary and the Department of Macroscopical and Clinical Anatomy, Medical University of Graz, Austria.

This thesis is a result of a collaboration of the author with colleagues of two universities, the Semmelweis University, Budapest (Hungary) and the Medical University of Graz, Graz (Austria).

I would like to thank my tutor, Professor Péter Windisch, and my mentors Dr. Bálint Molnár, Dr. Georg Feigl, Dr. Gábor Gerber and Dr. Andrea Dorottya Székely for their guidance and advice. I would like to express my sincere gratitude to my co-workers Dr. András Grimm, Dr. Dániel Palkovics and Dr. Gábor Baksa. I am grateful to Dr. Mark Eyre and Dr. Szilvia Mézey for their help and support during my PhD studies. I would also like to thank the staff of the Departments of Periodontology and Anatomy, Histology and Embryology of Semmelweis University and the Department of Anatomy of the Medical University of Graz.

Last, but not least, I would like to thank my loving family, my parents and my grandparents for their understanding and support during these years.